Fuel 324 (2022) 124711

Contents lists available at ScienceDirect

Fuel

journal homepage: www.elsevier.com/locate/fuel

Full Length Article

Intrinsic characteristics of coal combustion residues and their environmental impacts: A case study for Bangladesh

Abdul Baquee Khan Majlis [a], Md. Ahosan Habib [a,b], Rahat Khan [c,*], Khamphe Phoungthong [a,d], Kuaanan Techato [a,d,*], Md Aminul Islam [e], Satoru Nakashima [f], Abu Reza Md. Towfiqul Islam [g], Madison M. Hood [h], James C. Hower [h]

[a] Environmental Assessment and Technology for Hazardous Waste Management Research Center, Faculty of Environmental Management, Prince of Songkla University, Hat Yai, Songkhla 90112, Thailand
[b] Geological Survey of Bangladesh, Segunbaghicha, Dhaka 1000, Bangladesh
[c] Institute of Nuclear Science and Technology, Bangladesh Atomic Energy Commission, Savar, Dhaka 1349, Bangladesh
[d] Faculty of Environmental Management, Prince of Songkla University, Songkhla 90112, Thailand
[e] Department of Geosciences, Faculty of Science, University Brunei Darussalam, Gadong BE1410, Brunei
[f] Radioactivity Environmental Protection Course, Phoenix Leader Education Program, Hiroshima University, 1-1-1 Kagamiyama, Higashi-Hiroshima 739-8524, Japan
[g] Department of Disaster Management, Begum Rokeya University, Rangpur 5400, Bangladesh
[h] Center for Applied Energy Research, University of Kentucky, 2540 Research Park Drive, Lexington, KY 40511, USA

ARTICLE INFO

Keywords:
Fly ash
Bottom ash
Barapukuria power-plant, Bangladesh
Comprehensive characterization
Environmental impacts
Ecological and radiological risks

ABSTRACT

This study has focused on petrography, geochemistry, radiochemical, and leaching properties of coal combustion residues (CCRs), their leachates and nearby waters from the Barapukuria coal-fired power-plant (BCPP) to evaluate the potential environmental impacts and human health hazards for the first in Bangladesh. The CCRs, used in this study are predominantly comprised of Al-Si-rich glassy materials (94.8%) followed by crystallites (3.6%), notably quartz, mullite, and spinel with rock-fragments (0.3%); and un-burnt organic constituents (1.3%) such as anisotropic coke (0.8%) and slightly altered inertinite (0.5%). Hematite, magnetite, cristobalite, monazite, zircon, rutile, tourmaline and sillimanite were also identified as trace minerals. Elemental contents are found to be elevated (2.1–14.2 times) in the fly ash (FA) and bottom ash (BA), as compared to world coal-ash average with the exceptions of Ni in FA; and of Zn, As, Cu, and Hg in BA. The sum of detected rare earth elements is significantly high as compared to the world FA, Indian and Chinese ash residues. The specific activities of CCR are comparatively higher by a factor of 3.7 (^{226}Ra) to 6.2 (^{232}Th) than those of the world average. The examined spheres, particles, and agglomerates of FA are predominantly comprised of C, Al, and Si as major while, K, Ca, Mg, Fe, W and Ti as minor elements. On the other hand, extractable amounts of soluble potentially toxic elements in FA leachates are 7.7% for Se, 4.8% for Zn, and in BA 5.7% for As and 3.1% for Se and others are $< 1\%$. Metals are substantially released from FA in the range of 8.5 (for Cr) to 9650 (for Zn) ppb and 0.002% (for Cr) −7.7% (for Se), while from BA below detection level (for Cr) to 940 ppb (for Mn). The concentration of hazardous metals in the discharged waste water and water ash pond were higher than those were found in nearby pond- and ground-water sources around the BCPP. Ecological and radiological risk indices suggest moderate-risk derived from FA and low-risk from BA.

1. Introduction

Coal is, solid fossil fuel, identified as a source of primary energy and coal combustion activity is the primary means of power generation in many countries for a long time [1–3]. As the continuous growing demand for energy, annually a large quantity of coals are burnt in many countries, giving rise to huge amounts of coal combustion residues (CCRs: a collective term for fly ash, FA and Bottom ash, BA; herein after) from coal power-stations [4–6]. CCRs are globally regarded as an industrial waste, ecological nuisance and a Group I human carcinogen

* Corresponding authors at: Environmental Assessment and Technology for Hazardous Waste Management Research Center, Faculty of Environmental Management, Prince of Songkla University, Hat Yai, Songkhla 90112, Thailand (K. Techato).
E-mail addresses: rahatkhan.baec@gmail.com (R. Khan), uhugua@hotmail.com (K. Techato).

https://doi.org/10.1016/j.fuel.2022.124711
Received 7 November 2021; Received in revised form 26 March 2022; Accepted 27 May 2022

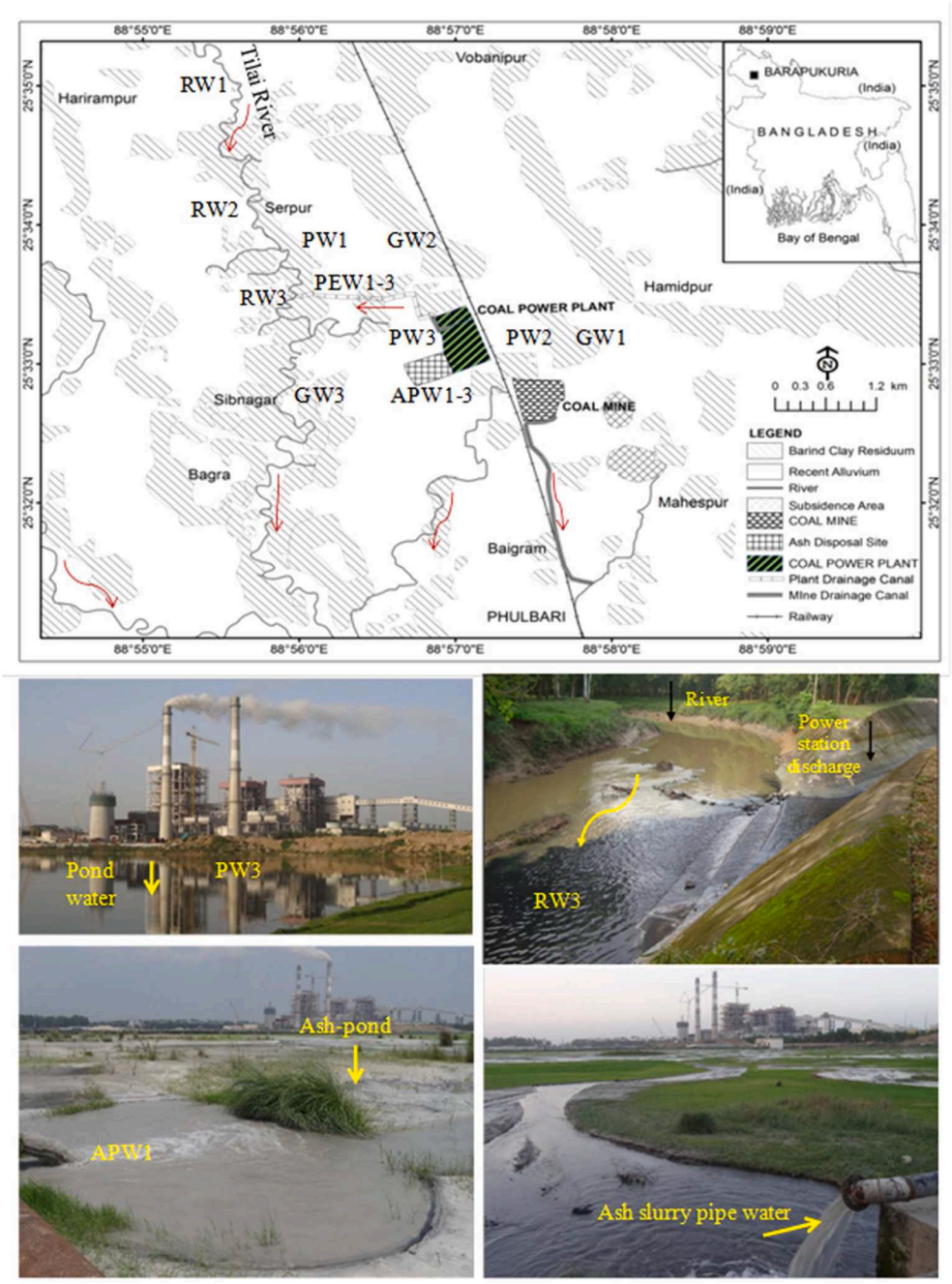

Fig. 1. Map showing the Barapukuria coal-fired power plant in Dinajpur, Bangladesh. Arrow (red) indicated flowing direction and yellow marked indicated water sampling points. GW: groundwater; PW: pond water; APW: ash-pond water; and PEW: power-plant effluent/discharge water. (For interpretation of the references to colour in this figure legend, the reader is referred to the web version of this article.)

[7–9] or a valuable raw material [6,10], some of which possess higher added value (e.g., Ga, V, REE, and U) [11] and could be recovered commercially and might be used as recoverable resources [12–13]. While others, such as Ba, As, Cd, Cu, Cr, Ni, Sb, Pb, Zn, Se, Hg, ^{226}Ra, ^{232}Th, and ^{40}K, are of definitely potential environmental concerns upon their release into the ambient nature [10,14,15]. Classification of environmentally sensitive trace metals [16] associated with the coal utilization are: (1) greatest concern (As, Hg, Cd, Pb, Se), (2) moderate concern (Cr, Cu, Ni, V, Zn), (3) minor concern (Ba Co, Mn, Sb), (4) radioactive (U, Th, K), and (5) hazardous air pollutants (As, Sb, Cd, Co, Cr, Pb, Hg, Mn, Ni, Se, U). According to Izquierdo and Querol, [17], CCRs is considered as a significant potential source which releases several environmentally sensitive elements [18]. Nevertheless, coal power-plant is one of the most significant sources of hazardous contaminants and treated as the biggest hazards to the nature [19]. In Bangladesh, study of the CCRs, in terms of the occupational stochastic effects, environmental and potential human health risk of hazardous toxic trace elements, radionuclides, unburnt carbons, and atmospheric particulates issues are scarce in literature, though similar studies having different geographical origin have been extensively investigated. Thus, it is of economic, ecological and environmental significance to evaluate its quality detail focusing on their potential utilization and probable hazard management.

Ash petrology provides information about the contribution and forms of chars and other inorganic constituents [20–22]. It may be useful in forecasting the leaching of hazardous metals, radionuclides,

Table 1
Petrographic compositions [in %] of the examined samples and comparison with other studies.

	This study									Literature data		
	FA 1	FA 2	FA 3	FA_{av}	BA 1	BA 2	BA 3	BA_{av}	FA[a]	BA[a]	FA[b]	FA[c]
1 Glass	94.9	96.2	95.0	95.4	94.0	95.3	90.0	93.1	68.0	79.0	97.2	48.0–89.0
2 Mullite	0.0	0.0	0.0	0.0	0.0	0.0	0.0	0.0	0.0	0.0	0.0	3.2–40.0
3 Spinel	2.9	1.3	1.9	2.0	4.1	1.9	3.6	3.2	8.0	2.5	trace	na
4 Quartz	trace	0.3	1.1	0.49	1.4	2.0	1.0	1.5	0.8	8.0	0.4	1.7–12.5
5 Sulfide	0.0	0.0	0.0	0.0	0.0	0.0	0.39	0.13	na	na	na	na
6 Rock fragments	1.1	0.31	0.0	0.47	0.0	0.0	2.0	0.67	0.0	0.5	1.6	na
Total inorganic	98.9	98.1	98.1	98.4	99.5	99.1	97.0	98.6	**76.8**	**90.0**		
7 Isotropic coke	0.0	0.0	0.0	0.0	0.0	0.0	1.7	0.39	na	na	na	na
8 Anisotropic coke	0.72	0.94	0.76	0.81	0.46	0.39	0.40	0.42	2.0	5.5	0.4	na
9 Inertinite	0.36	0.94	1.1	0.82	0.0	0.47	0.88	0.68	4.0	3.0	0.4	na
Total organic	1.1	1.9	1.9	1.6	0.46	0.86	3.0	1.5	**6.0**	**8.5**	**0.8**	

na: Not available; fly ash (FA); bottom ash (BA). Neoformed (1, 2, 3, 7, 8) from (in)organic and coal derived (4, 5, 6, 9).
[a] [23], Indian FA and BA.
[b] [57], Jungar, China, minus-500 fractioned-sized FA.
[c] [69], European FA.

and potentially harmful bio-reactive organic compounds (e.g., PAHs, UCs) [10,23]. In fact, spheres and chars containing enhanced harmful pollutants are the significant contributors of contaminants [17] and a source of risks to human health, ecology and environment [7,8,24]. As environmental consciousness increases, there is also a growing tendency of recycling of CCRs in multi-sectors throughout the world [25]. However, a large amount is still unused and improperly dumped, thereby, easily releasing dreadful environmental contaminants and subsequently leading to serious contaminations, health risks and affecting the ecosystem [6,26]. The uncontrolled disposal of these CCRs leads to significant environmental problems [27]. Much of the residues are dumped in the ash ponds (lagoons) with routine effluent discharges that reach to nearby water sources. If the settling pond is unlined, then a large volume of the leachate migrates and gradually percolate downward leading to affect nearby water table and drinking water sources [27]. Only geochemical investigations are not enough to describe the complexity of CCRs completely. For instance, the forms of carbons and their relationship to the inorganic residues constituents; the burnout of coal and non-coal carbons; and the combustion efficiency, can all be explained by petrographic characterization of residues [21]. The main harmful aspect is that the contaminants particularly heavy metals, radionuclides, rare earth elements (REE), and chars contained in the produced CCRs are likely to be readily liberated and directly migrated and remobilized into the environment from producing and disposal sources in diverse modes [17,28–30]. Chars are potentially harmful bio-reactive contaminants and associated with other toxic elements [23]. Toxicological research has shown that CCRs is carcinogens, endocrine disruptors, and cardiorespiratory toxins [7,31]. In addition, it is of great concern as these contaminants are dispersed in a very wide range of the nearby natural systems. Accordingly, it may modify the natural background compositions of ambient environmental components/media e.g., soils, waters, sediments. Consequently, it may adsorb, retain, and consequently transfer to plants/crops. Finally, these contaminants may expose to humans, vegetation and other living beings leading to cause adverse environmental issues and acute health diseases via various possible exposure routes [26,32–34]. Therefore, if CCR is not disposed of properly, maintained scientifically, study and monitor regularly, serious and long-lasting environmental and health hazards and disruption of ecological cycles, could arise [35–37]. Thus, it is critical to characterize CCR properties.

Comprehensive characterization and speciation of CCRs from a Barapukuria coal power-station (BCPP) in Bangladesh is a quite new initiative for evaluating its prospects, challenges and suitable exploration and management strategies. Although the abundances of diverse elements can greatly be varied in CCRs produced even within a specific region, there are some typical trends in their composition from different countries. Thus, it is imperative for a better understanding of the concentration, distribution, behavior and occurrences of precious and poisonous constituents for optimum utilization and sustainable management. As like other South-Asian countries and other developing countries, there is remarkably raised power generation through both domestic and international sourced coal-burning and simultaneously increased significantly ash production in the country. It is also anticipated that the production of CCRs would be considerably increased in the successive years [3] and would steadily elevate environmental concerns. Though, a number of coal-based power-plants (1,320 MW, each) development projects are in implementation. Currently, the BCPP (525 MW) is consuming indigenous Permian Gondwana coals (inertinite-rich bituminous) from nearby underground Barapukuria coal field as feedstock and the produced CCRs of are inappropriately stored in stockpiles and ash-repositories temporarily, and finally are disposed of in open and unlined ash-ponds. It is located in a (population density: 823/km^2) multi-cropped agricultural and humid subtropical region in alluvial-fluvial floodplain system in NW region of the country [33]. At present, the wastewater and discharge of the power-station and ash-ponds drainage channel are directly drained to the Tilai River (Fig. 1). Though, the study of the CCRs in many countries regarding their economic prospects and corresponding impacts on environment have been extensively investigated and reviewed [8,36,38] while from the BCPP, are scarce in literature and the potential economic prospects, beneficial uses, and environmental threats none of these issues have not yet scientifically been characterized so far. Under such circumstances, sustainable management of CCR in socio-economic and environmental context through detailed speciation and characterization would be an inevitable concern. Furthermore, the contributions to the application of potential hazard mitigation measures and further reduction of handling costs, protection from probable contamination and adverse effects are also prime concerns. Moreover, this study can reinforce the environmental legislation, sustainability, and proper implementation of remedies.

The primary objectives of the present research are to: (1) characterize the ash petrography; (2) assess abundance and distribution of the elemental and natural radionuclides in CCRs; (3) determine the potential leachability of some selected heavy elements; and (4) evaluate the potential risk of potentially toxic elements (PHEs) leached from CCR to the environment. The results of the present research may provide information which, can be employed to environmental impact assessments.

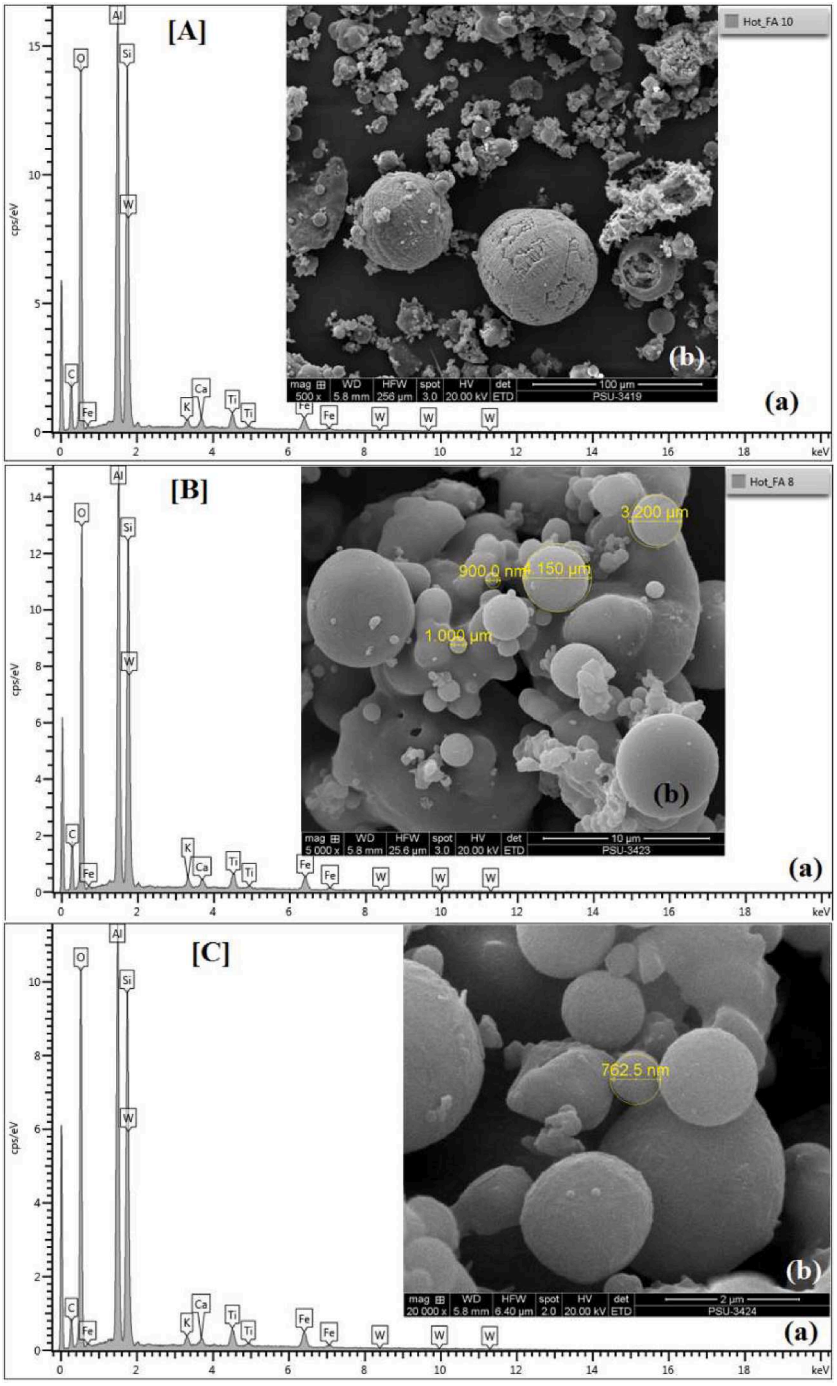

Fig. 2. SEM-EDS photomicrographs represent an overview of micromorphology of the fly ash (FA) samples. Predominantly fused Al-Si-rich glassy matrix with spherules, particles, agglomerates, and unburnt (in) organic constituents. [A] (b) Magnetite sphere with mosaic fabric, plerosphere, and other metallic and glassy spherical particles. [B](b) Spherule with smooth orange-peel surface structure; spherical and irregular molted grains hollow cenospheres with porous particles. [C] Glass cenospheres, respirable size particles. Surface composition of ash-particles appears in table (Supplementary information: Table S2). (For interpretation of the references to colour in this figure legend, the reader is referred to the web version of this article.)

2. Experimental and methodology

2.1. Sampling and sample preparation

The BCPP combusts around 0.72 million tons of Permian aged Gondwana coal (highly-volatile inertinite-rich bituminous B ranked) to generate electricity and subsequently generates and dumps nearly 0.08 million tons of high-quality solid byproducts per annum of which, 80% is approximated to be FA and the rest is BA. These are directly sluiced to the nearby open disposal sites i.e., ash ponds mixed with water, which are already filled and flowed with water to affect nearby crop lands and minimal portions are used as filled materials in depression or low land, and cement factories. The samples of FA (electrostatic precipitators, ESP hoper) and BA (tank) of the BCPP Unit-1 (FA 1 & BA 1) and Unit-2 (FA 2 & BA 2) were simultaneously sampled through a scientific procedure at ten different times (i.e., ten sub-samples for each item from same location). Additionally, FA 3 and BA 3 samples were also collected randomly from the composite output going to the temporary ash-repositories of the power-plant site. All collected samples were put in Ziploc plastic bags immediately and sealed carefully to minimize possible oxidation and contamination. In order to prepare composite, more representative and bias-free samples and to reduce the number of samples, for each item of the same type, ~250 g of dried (with exception of samples for Hg test) subsets of the samples (ten for each item) were then thoroughly and homogeneously mixed. And then the samples were milled (with exception of samples for grain size experiment), coned and quartered into representative portions for subsequent tests, except FA, which was in very fine-grained form. Each item of the same type composite samples

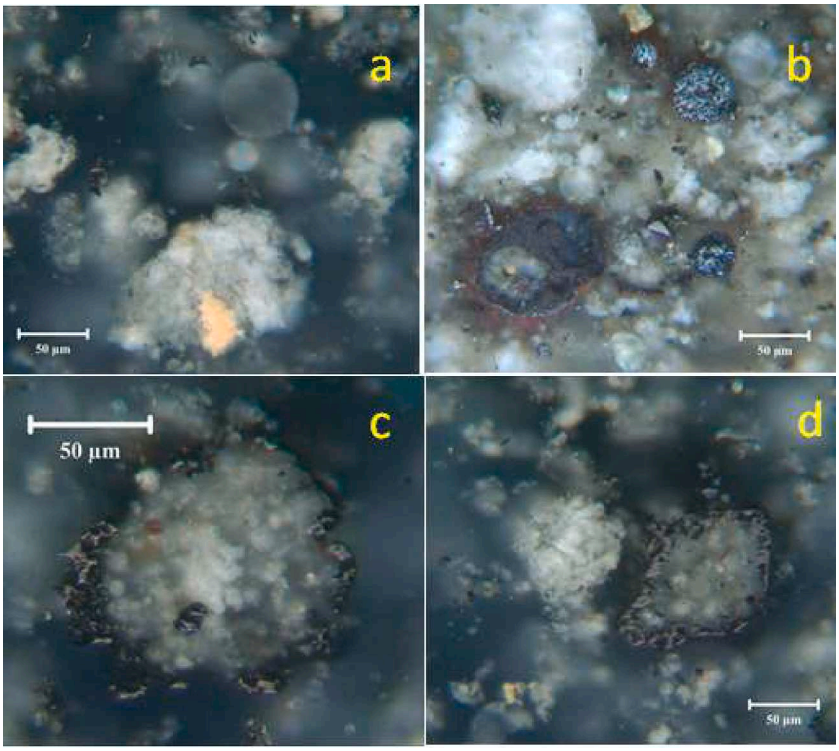

Fig. 3. Neoformed glass materials in the FA samples. (a) Glassy matrix with solid and glassy spheres, (b) Glass with spinel, tiny fragments of coke, and minerals embedded in fused rock-fragments with exterior thin, red oxidation rim, (c-d) Core glassy constituents with isotropic and anisotropic coke in outer sphere. (For interpretation of the references to colour in this figure legend, the reader is referred to the web version of this article.)

were then homogenized and re-sampled as required and split for subsequent laboratory experiments. A total of 15 composite water samples were also collected from different water sources (indicated in Fig. 1) around power-station (pond water: PW1-3; plant effluent discharge water: PEW1-3; groundwater/power-station-intake water: GW1-3, ash-pond water: APW1-3; river water: RW1-3) and subsequently analyzed.

2.2. Sample analysis

2.2.1. Physical properties analysis

The pH of the CCR samples was determined in distilled water using a digital pH meter (Inesa, PHS-2F, China) following the standard protocol [4]. The pH and conductivity of the samples were measured by conventional methods. Granulometric distributions of the un-milled raw samples were carried out by Laser particle size analyzer (LS 230, Coulter, USA).

2.2.2. Petrographic analysis

The CCR samples were fixed in epoxy; prepared to a final 0.05-µm polish; and investigated using microscopy (reflected light, oil-immersion optics). Detail description of the characterization technique was similar to those of previous studies [38].

2.2.3. Chemical composition analysis

The major elements (3 oxides: SiO_2, MgO, CaO) of the CCR samples were analyzed by X-ray Fluorescence (XRF: PW 2400, Philips, Netherlands). Approximately 0.3 g of each prepared samples was taken in a porcelain crucible and were then milled with binder (wax: sample, 1:3) followed by shaking for 2 h. Resulting mixture was spooned into an aluminum cap (30 mm) which was then sandwiched between two tungsten carbide pellets. Finally, the pellet was ready for subsequent XRF analysis.

On the other hand, bulk chemical compositions of Al, Fe, Ti, Na, K, Sc, V, Cr, Mn, Co, Ga, Zn, As, Rb, Br, Sb, Ba, Cs, La, Ce, Yb, Sm, Eu, Lu, Hf, Ta, W, Th, and U of the ash samples were performed by instrumental neutron activation analysis (INAA) following the established process [39–43]. Briefly, a certain quantity (50 mg, oven dried) of the samples were weighed and heat-sealed in high purity polyethylene bag. Samples were then irradiated by neutron using 3-MW TRIGA Mark-II research reactor (Bangladesh Atomic Energy Commission) followed by gamma counting (HPGe detector) with systematic cooling. Relative standardization approach was used for the accurate and precise measurement of elemental contents [43,44].

However, Cd, Cu, Ni, Pb, and Se abundances in the CCRs were determined by Inductively Coupled Plasma Optical Emission Spectroscopy (ICP-OES: Optima 800, Perkin Elmer Instruments, USA) by following the standard method [4,36,44]. About 0.5 g of the CCR sample was weighed in replicate and transferred to a Teflon flask containing an acid mixture of (3:3:2) concentrated HCl–HNO_3–HF. Consequently, the flask was tightly closed and heated in a closed vessel microwave system following US ASTM protocol [45]. Subsequently the resulting solution was poured into a 100 mL volumetric flask after cooling to room temperature, followed by dilution to a constant volume with de-ionized water. Finally, the abundance of concern metals of interest in the resulting extract was determined by means of ICP-OES. Furthermore, mercury analyzer (FIMS 200, Perkin Elmer) was utilized to determine Hg content in the raw CCR samples.

2.2.4. Radioactivity measurements

Radioactivity concentration of NORMs (^{226}Ra, ^{232}Th, and ^{40}K) in the CCRs were determined by Gamma-ray spectrometry with a low-background high-purity germanium detector (GEM 30–70, ORTEC, Japan) following the standard protocol [32,33]. Concisely, hermetically filed samples (~250 g) were counted for ~ 45000 s by HPGe detector after attaining the secular equilibrium (28 days) among the short- and long-lived decay products.

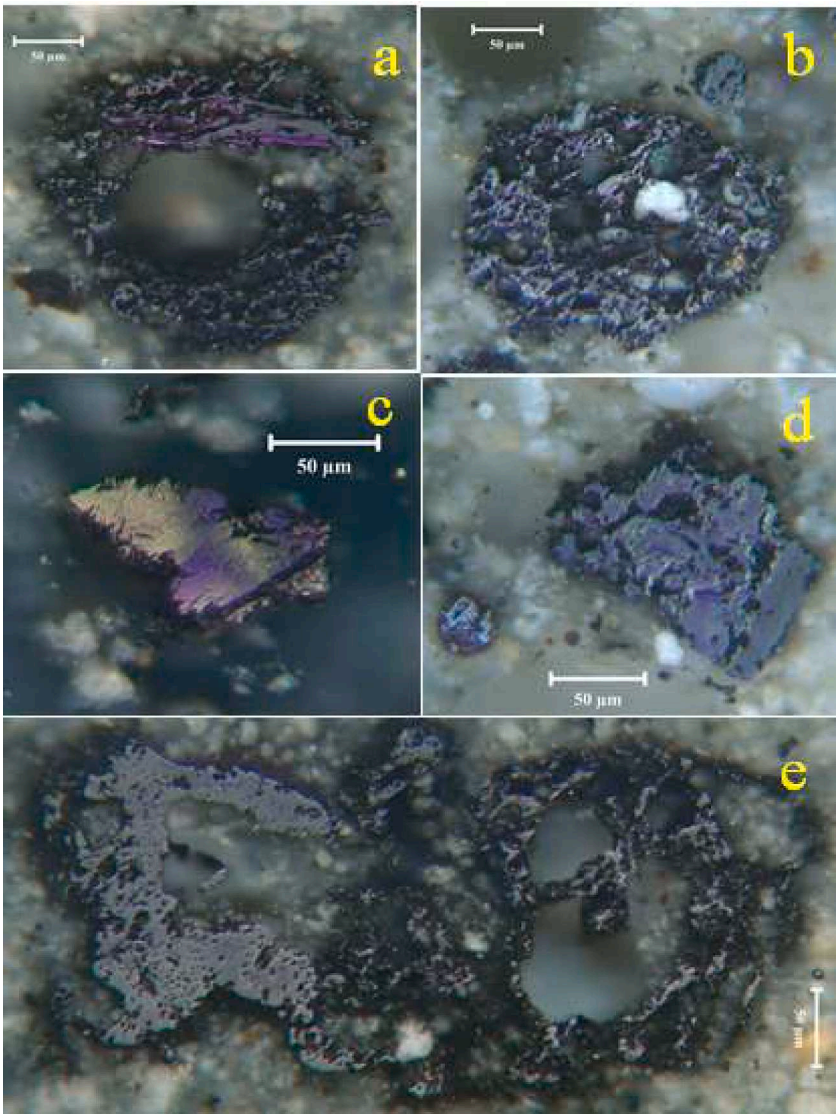

Fig. 4. Photomicrographs of unburnt organic constituents i.e., carbon in the FA samples examined. (a-b) massive to porous transformed dense anisotropic in crassisphere with inertinite (honeycombs view) showing remnant cell structure. (c-d) massive inertinite debris with surrounding glass, (e) anisotropic coke with inertinite.

2.2.5. Mineralogical and Micro-morphological analysis

Mineralogical study was conducted by X-ray Diffraction (XRD: X-Pert MPD, Philips, Netherlands). Briefly, ~1 g of CCR samples were packed into a steel cavity mounts which were appropriate for insertion into diffractometer. Then XRD spectra were recorded by using a diffractometer with Cu-Kα radiation (scan range (2θ) of 2–90°, nickel filter, 40 kV, 30 mA amperes and 3°/min diffraction speed). Additionally, semi-quantitative optical microscopic study was also carried out to estimate the modal abundances of minerals in CCR materials. In doing so, some epoxy was taken on a glass slide and kept on the heater. While it was melted, the samples were sprinkled on the liquid. Afterward, a cover glass was put on this mixture and pressed until the extra epoxy and bubbles were removed. After cooling the slide, it was cleaned by xylene & cotton, and was ready for microscopic study (ZEISS Axio Scope.A1, Germany).

However, Fourier Transform Infra-red spectroscopy (FTIR: WI-RES-FTIR2-001; technique: Pellet KBr; VERTEX 70, Bruker, Germany) was used for micro-structural analysis. In doing so, ~1 mg of CCR samples were milled with spectroscopic grade KBr (1:100) with an agate mortar for 5 min; and subsequently compacted in a hand press pellet maker. Prepared pellets (thickness, 0.5 mm) were dried in an electric oven (at 105 °C) for 24 h before investigation. Then the pellets were attached in a holder and introduced in the IR beam of the spectrometer. Additionally, the micromorphology of the ash particles were also investigated with Scanning Electron Microscope (SEM: Quanta400, FEI, and Czech Republic) coupled with Energy Dispersive Spectroscopy (EDS: X-Max, Oxford, England). The EDS was applied to determine surface chemical composition. The materials (around 0.9 g) were prepared into pellets and mounted on standard Al stubs with carbon tape. The SEM-EDS working distance was set at 10 mm with the beam voltage of 20 kV.

2.2.6. Leaching test

The Toxicity Characteristic Leaching Procedure (TCLP) was carried out in order to determine the potential leachability of selected elements, namely, Ba, Cd, As, Se, Cr, Cu, Mn, Ni, Pb, and Zn [37,46] and the possibility of transferring those elements to the environmental media [47]. The sample (about 5 g, each) was first mixed with (buffered) acetic acid in a high-density polyethylene bottle at a sample-extraction fluid ratio of 1:20. The mixture (bottle) was continuously stirred end-over-end at a speed of 30 ± 2 rpm for 24 h at room temperature. Thereafter the eluate was then filtered at 0.45 µm. Finally, the concentration of concerned metals was determined in the resulting leaching extract

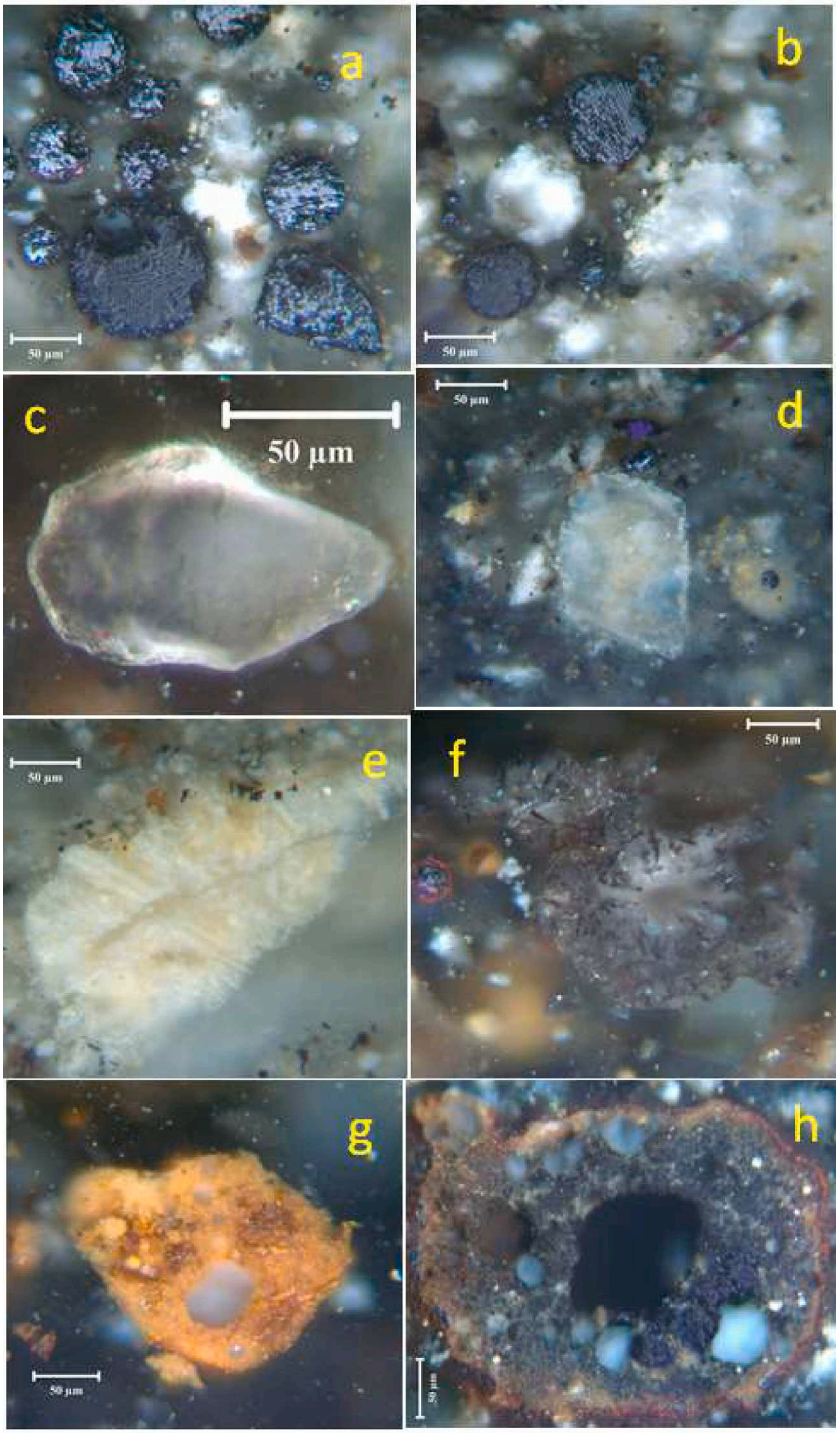

Fig. 5. Relict, fused, and melted inorganic constituents in the bottom ash (BA) samples. (a-b) Spinel spheres presumably magnetite/hematite and mullite laths in glassy matrix; (c-d) Angular quartz particles showing smoky character, sub-angular mineral grain embedded in amorphous glassy matrix; (e-f) Needle like neoformed acicular mullite in glass; (g-h) Baked-rocks with bladed crystallites and vitrified outer edge, Fe-oxidation.

using ICP-OES [4,48]. Independent duplicate measurements of resulting extracts were performed under the same analytical conditions in all the cases to ensure the data quality.

2.2.7. *Water sample analysis*

Water quality parameters, e.g., SO_4^{2-}, Ca, Mg, Na, K, Se, Ba, Ni, Zn, Cu, Fe, Pb, Mn, Cr, Cd, As, and Hg were measured in the collected samples. Sample collection, processing and instrumental analysis of measured parameters were essentially the same as that of our previous study [34]. Briefly, cations in water samples were measured by flame atomic absorption spectrometer (FAAS, Perkin Elmer AAnalyst 400, USA) after acid digestion and required dilutions following standard protocol [49–51] here as non-acidified water samples were utilized for SO_4^{2-} analysis using an Ion Chromatograph (Model: SIC10AVP, Shimadzu, Japan) following standard guidelines [52,53].

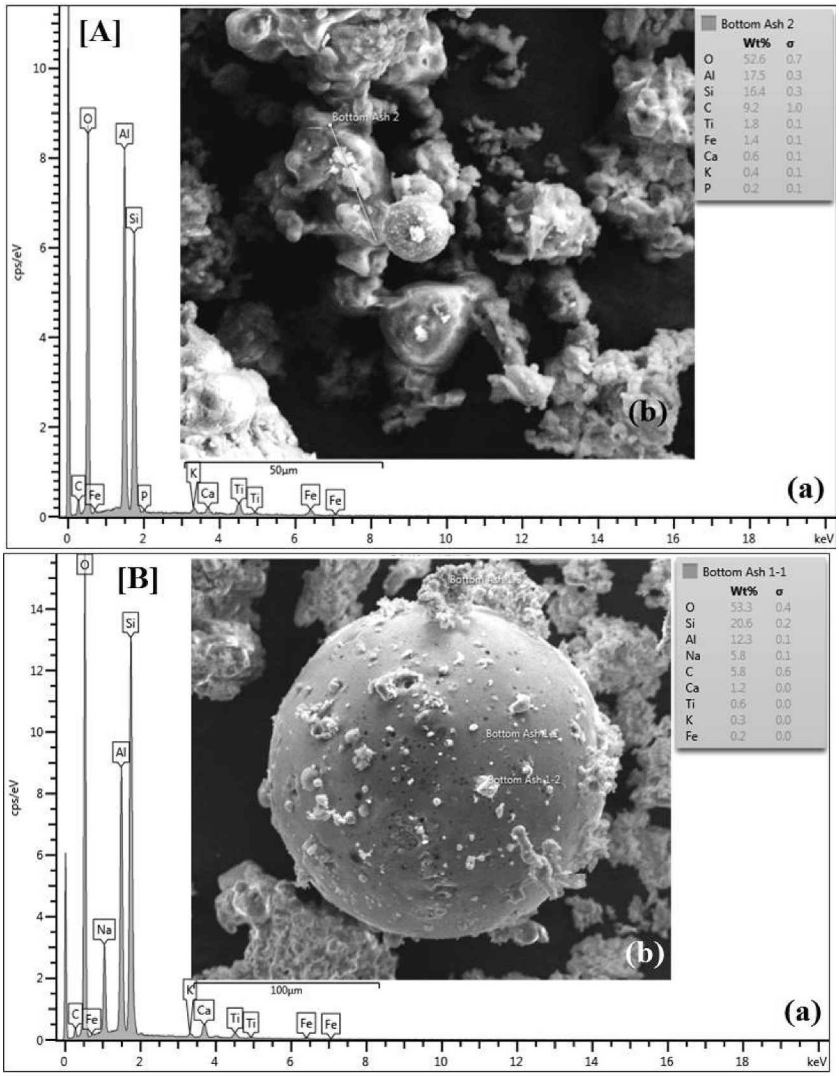

Fig. 6. SEM-EDS images with spectra of the BA samples. Predominantly Si-Al glassy matrix with unburnt carbon. Surface composition of ash-particles appears in table (Supplementary information: Table S2).

2.3. Ecological and radiological hazard indices

According to Hakanson [54], potential ecological risk index (RI) was employed to evaluate the extent of pollution of the toxic and hazardous elements such as As, Cd, Cr, Cu, Mn, Ni, Pb, and Zn in CCR samples. The formula (Eq. 1) for estimating the RI, is as follows:

$$RI = \sum_{i=1}^{n} Er^i = \sum_{i=1}^{n} Tr^i \times Cf^i \quad (1)$$

where, $\sum Er^i$ is the sum of the potential ecological risk factor of selected potentially toxic elements; Cf is the contamination factor, $Cf^i = Cm/Cb$, where Cm is the concentration of an individual element in the sample; Cb is the background content of the elements in UCC; and Tr^i is biological toxic metal response factor of an individual hazardous metal [54]. Based on the Er^i and RI values, risks were categorized into three classes: Class 1: low risk ($Er < 40$ and $RI < 150$); Class 2: considerable risk ($80 \leq Er \leq 160$ and $300 \leq RI \leq 600$); Class 3: very high risk ($Er > 320$ and $RI > 600$), respectively [55]. However, methodologies and mathematical expressions for radiological indices, e.g., Radium equivalent activity, $Ra_{eq} = \left(\frac{A_{Ra}}{370} + \frac{A_{Th}}{259} + \frac{A_k}{4810}\right) \times 370$, and Hazard index, $H_{ex} = \frac{A_{Ra}}{370} + \frac{A_{Th}}{259} + \frac{A_k}{4810}$ for considered natural radionuclides are same as those of [32,33], where A_{Ra}, A_{Th} and A_K are activity concentrations (in $Bq.kg^{-1}$) of ^{226}Ra, ^{232}Th, and ^{40}K, respectively.

3. Results and discussion

3.1. Textural and petrographic characterization of CCRs

The size distribution of the samples is illustrated in Fig. S1. The average, size of FA-particles is 53.0 μm with $D_{10} = 9.5$, $D_{50} = 34.9$, and $D_{90} = 129.0$ μm while the mean value of BA is 730.9 with $D_{10} = 116.0$, $D_{50} = 723.6$ and $D_{90} = 1389.0$ μm indicating coarser grain distribution. On the other hand, the results of petrographic examinations of CCR samples are tabulated in Table 1 and appeared in Figs. 2–6. The CCRs consist of a variety of components predominantly non-crystalline amorphous phase (glass component) (FA_{ave}: 95.4%, BA_{ave}: 94.1%) (Figs. 2 and 3), followed by lesser proportions of organic constituents (unburnt carbon or chars) (Fig. 4), other phases encompassing partially baked rock fragments with cokes or occasionally "glassy rims" (FA_{ave}: 0.7%, BA_{ave}: 0.4%), and a minor proportion of relict quartz, mullite and Fe-spinel (presumably magnetite) (Fig. 5). The char contents are 1.6% and 0.9% in the investigated FA_{ave} and BA_{ave}, respectively, with massive to porous residual anisotropic coke (crassisphere) [38,56] (FA_{ave}: 0.8%, BA_{ave}: 0.5%) and some inertinite (carbon particles) (FA_{ave}: 0.8%, BA_{ave}: 0.4%). However, these organic constituents are relatively lower than those available in Indian FA [23] but are comparable to those in Chinese FA [57]. Furthermore, SEM observation represents that glassy

Table 2
Elemental abundance in the examined samples and compared to world literature and limit data. All units are in ppm.

This study									EU	World	India		China		Australia		Limit	
	FA 1	FA 2	FA 3	FA_{av}	BA 1	BA 2	BA 3	BA_{av}	FA[a]	WCA[b]	FA[c]		FA[d]	BA[d]	FA[e]	BA[e]	China[f]	EU[g]
Sc	38.7	45.8	43.2	42.6	31.3	33.1	29.0	31.1	na	24	18.0–28.9		17.0	16.4	na	na		
V	180.1	188.1	228.6	198.9	153.7	137.0	136.9	142.5	154–414	170	100–164		68.3	63.8	180	76		
Cr	177.9	247.5	241.8	222.4	141.3	132.9	139.2	137.8	47–281	120	116–172		90.2	25.7	70	56	120	70
Mn	741.8	463.6	726.2	643.9	340.2	334.4	589.3	421.3	na	430	286–510		92.3	100.7	280	1031		
Co	12.2	21.3	24.2	19.2	7.2	10.6	5.6	7.8	20–112	37	17.6–20.3		2.9	21.4	20	9		
Ni	37	43	36	38.7	18.8	64.2	44.9	42.6	49–377	100	50.9–68.2		12.3	65.5	77	82	150	40
Cu	48.8	50	66	54.9	28.6	32.6	59.7	40.3	39–254	110	58.5–82.4		37.7	27.3	66	67	750	100
Zn	220.1	117.2	216.1	184.5	10.0	31.0	49.3	30.1	70.0–924.0	170	55.8–135.9		48.1	32.9	150	30	750	200
Ga	40.4	55.1	56.0	50.5	26.9	15.5	19.2	20.5	na	36	30.4–68.8		43.4	35.4	na	na		
As	3.2	5.7	10.8	6.6	0.95	0.54	0.75	0.75	22–162	46	<0.2–6.7		1.1	0.37	11	14	25	25
Se	0.88	0.72	0.55	0.72	0.72	0.33	0.24	0.43	3.0–30.0	10	0.7–4.4		3.6	0.96	6	1.1		7
Br	3.0	5.5	6.5	5.0	1.8	1.2	0.09	1.0	na	32	na		na	na				
Rb	53.5	60.7	49.3	54.5	42.8	29.4	41.3	37.8	22–202	110	59.5–87.2		8.5	8.8	97	17		
Cd	3.2	0.92	1.7	2.0	2.9	0.99	1.4	1.8	<1–6	1.2	0.16–0.65		0.1	0.09	0.9	0.6	5	5
Sb	2.1	3.3	3.8	3.1	0.78	0.78	0.66	0.74	1–120	7.5	0.46–1.3		0.45	0.32	3	1		
Cs	7.4	7.4	5.9	6.9	6.2	4.9	4.0	5.0	na	8	7.0–9.9		0.69	0.67	na	na		
Ba	454.8	641.5	630.6	575.6	404.5	581.6	681.2	555.8	311–3134	980	475–828		150.0	91.1	490	341	1500	300
La	150.2	184.6	174.0	169.6	103.9	116.1	115.6	111.9	na	76	na		62.2	75.4	na	na		
Ce	260.8	333.8	317.8	304.1	210.7	227.3	216.3	218.1	na	140	na		107.0	118.0	na	na		
Sm	21.5	24.5	23.3	23.1	14.5	23.7	18.0	18.7	na	14	na		8.0	9.6	na	na		
Eu	3.2	4.5	4.0	3.9	2.7	2.4	2.1	2.4	na	2.6	na		1.4	1.6	na	na		
Yb	8.3	8.6	8.2	8.4	7.4	8.3	7.9	7.9	na	6.9	na		4.1	4.4	na	na		
Lu	1.2	1.3	1.1	1.2	1.0	0.78	0.62	0.8	na	1.3	na		0.58	0.62	na	na		
Hf	16.6	17.7	17.5	17.3	14.5	21.0	22.6	19.4	na	9	1.7–4.8		24.4	20.6	na	na		
Ta	3.4	4.1	3.5	3.7	2.6	4.7	4.3	3.9	na	2	1.8–2.9		4.2	3.7	na	na		
W	7.6	13.6	18.5	13.2	6.9	13.1	12.2	10.7	na	7.8	3.6–8.9		4.8	242.0	na	na		
Hg	0.034	0.049	0.031	0.038	0.009	0.020	0.006	0.012	<0.01–1.3	0.87	286–510		0.05	0.01	na	na	2.5	
Pb	34.5	47.5	53.9	45.3	34.0	22.8	33.0	29.9	40–175	55	35.2–87.0		55.5	23.9	75	8	50	50
Th	49.0	57.7	53.6	53.4	38.5	44.4	39.3	40.7	17–65	23	26.3–40.9		37	44.8	na	na		
U	11.4	13.3	14.1	12.9	8.3	9.8	8.5	8.9	5–29	15	5.8–10.8		10.6	10.9	na	na		
∑REE	445.2	557.3	528.4	510.3	340.2	378.6	360.5	359.8	–	240.8	–		183.3	209.6	na	na		
Radioactivity	FA 1	FA 2	FA 3	FA_{av}	BA 1	BA 2	BA 3	BA_{av}		WFA[h]	India FA[i]	BA[i]	China FA[j]	BA[j]				Coal[h]
^{226}Ra	127	164.2	165.5	152.2	93	102.2	130.9	108.7		240	78.8	41.4	69.5	59.5				35
^{232}Th	179	233.7	231.2	214.6	132	156.1	188.1	158.7		70	61.7	24.4	79.3	61.8				30
^{40}K	132	156.1	188.1	158.7	239	149.6	183.9	190.8		265	99.1	9.5	233	222.6				400

∑REE: Sum of detected rare earth elements (La, Ce, Sm, Eu, Yb, Lu).
[a] [69]; European FA.
[b] [79]; WCA: World hard coal-ash average.
[c] [76]; Bokaro, Indian FA.
[d] [57]; Jungar raw FA and BA.
[e] [64]; ash derived from bituminous coal.
[f] [73]; Chinese hazardous limit.
[g] EU limit values [74] (European Council Decision 2003/33/CE for hazardous limit values of some toxic elements for landfill materials.
[h] [85]; for world coal and world fly ash- WFA.
[i] India FA and BA radioactivity [87].
[j] Xijiao, China FA and BA radioactivity [86].

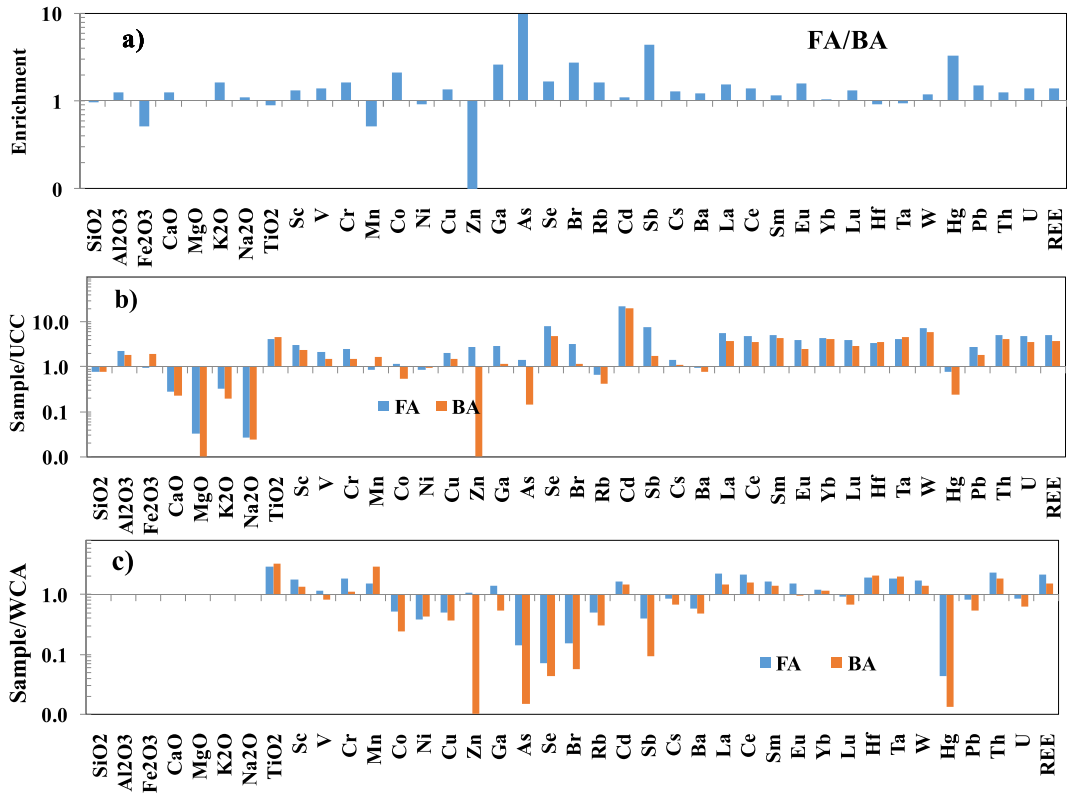

Fig.7. a) Major and trace-element ratios between FA-) and BA-samples. b) Distribution patterns of average values of major and trace elements in world hard coal-ash (WCA) [79], normalized to Upper Continental Crust (UCC, [70]) and WCA.

microspheres are the most abundant constituents in FA samples, and depicted by heterogeneous combination of agglomerates and spheres composed of particularly cenospheres (either dense or hollow) (Fig. 2), plerospheres (typically impregnated by smaller cenospheres), magnetospheres irregular debris (Fig. 2A-b). Comparison of FA morphotypes shows that the BA materials are composed of large angular shards/fragments with only a small proportion of semispherical particles. Similar observations are also reported by many researchers [19–21,58,59]. However, in the feeding coal (bituminous) of Barapukuria, contents (in wt. %) of ash, moisture, volatile matter, fixed carbon, carbon, hydrogen, nitrogen, oxygen, vitrinite, liptinite, inertinite, mineral matter, and vitrinite reflectance were 8.9–28.3, 3.1–5.3, 25.8–33.1, 45.9–62.1, 81.8–84.6, 5.0–5.2, 1.6–1.8, 8.1–10.7, 26.4–47.6, 3.7–8.9, 48.7–66.7, 6.7–14.5, and 0.71–0.78, respectively with less amount of total sulfur (0.63–0.71%) [60–63].

3.2. Mineralogical and structural properties

Mineralogical compositions of the CCR samples are mainly quartz (Fig. 5c, d), mullite (Fig. 5f), cristobalite, magnetite, and spinel (Fig. 3b; 5a, b) which are detected through XRD analysis (Fig. S2) and microscopic study. In the finest FA matrices, the crystals occurred either encapsulated in Al-Si-Fe-Ti rich glassy matrices or as discrete crystals as identical with previous demonstrations [4,64,65]. The Fe-sulfides (e.g., pyrite) present in feeding-coals are oxidized to form Fe-oxides (e.g., hematite, magnetite, maghemite, spinel) [20,21], whereas quartz remains unaltered during combustion or partially recrystallized from the silicate melt. Clays (e.g., kaolinite, illite) undergoes several intermediate changes before forming mullite [31,66,67]. The $SiO_2/Al_2O_3/CaO$ ratio in the glassy materials is critical to favor mullite crystallization. Alternatively, cristobalite may directly be recrystallized from the silicate melt [6]. Under optical microscope, some accessory resistant minerals are identified in BA samples as relict crystals including monazite, rutile, zircon, tourmaline, sillimanite and spinel (Fig. S3) which are derived from feed-coal.

In FTIR study the observed bands are 3442.1, 1097.9, 897.5, 744.8, 563.3 and 463.3 cm^{-1} in FA; while 3451.7, 1637.3, 1098.0, 894.4, 807.1, 732.5, 606.6, 557.3 and 463.9 cm^{-1} in BA, respectively (Fig. S4). The strong, broad band at 3442 and 3451.7 cm^{-1} typically belongs to O–H groups and the weak frequency peak at 1637 cm^{-1} is usually characteristic of the H-O–H bending mode. The analyses reveal that peaks occur around 1100 and 400 cm^{-1} for both O–H and the Si-O-Si, and Si-O-Al stretching vibration modes which are likely associated with fused alumosilicate and silicate phases (e.g., mullite, quartz, cristobalite) and amorphous glassy-matrices [4]. The peaks at 563 and 557 cm^{-1} are possibly due to the presence of Fe-oxides minerals. These results are consistent with the observations made from XRD findings (Fig. S1). The detection peaks at 3442.1 and 3451.7 cm^{-1} are an indication of the presence of N–H and –OH (stretch) groups. Appearance of a frequency peak at 2920.7 cm^{-1} indicates the presence of aliphatic > CH_2 group in the analyzed samples. The frequency peaks 897.5, 894.4, 807.1, 744.8, and 732.5 cm^{-1} may give the information of ring sizes of polyaromatic substances' stretching aromatic C═C and C–H vibrations. The peaks at 1637.3 and 1624.7 cm^{-1} are due to the presence of stretching aromatic C═C group/OH stretching vibration of coordinated water or bonded –OH. The peaks at 1098 and 1097.9 cm^{-1} are likely due to the occurrence of C–O bond. The bands at 563.3, 463.9, and 463.3 cm^{-1}occur in the samples which are likely due to the stretching vibration of S-S bond. Peaks ~ 1600 and 700–900 cm^{-1} support the occurrence of aromatic ring frequency out of plane vibrations of aromatic C–H bonds, rather than minerals [4].

3.3. Geochemistry of CCRs

3.3.1. Major oxides

Elemental distribution in FA and BA examined in this work and

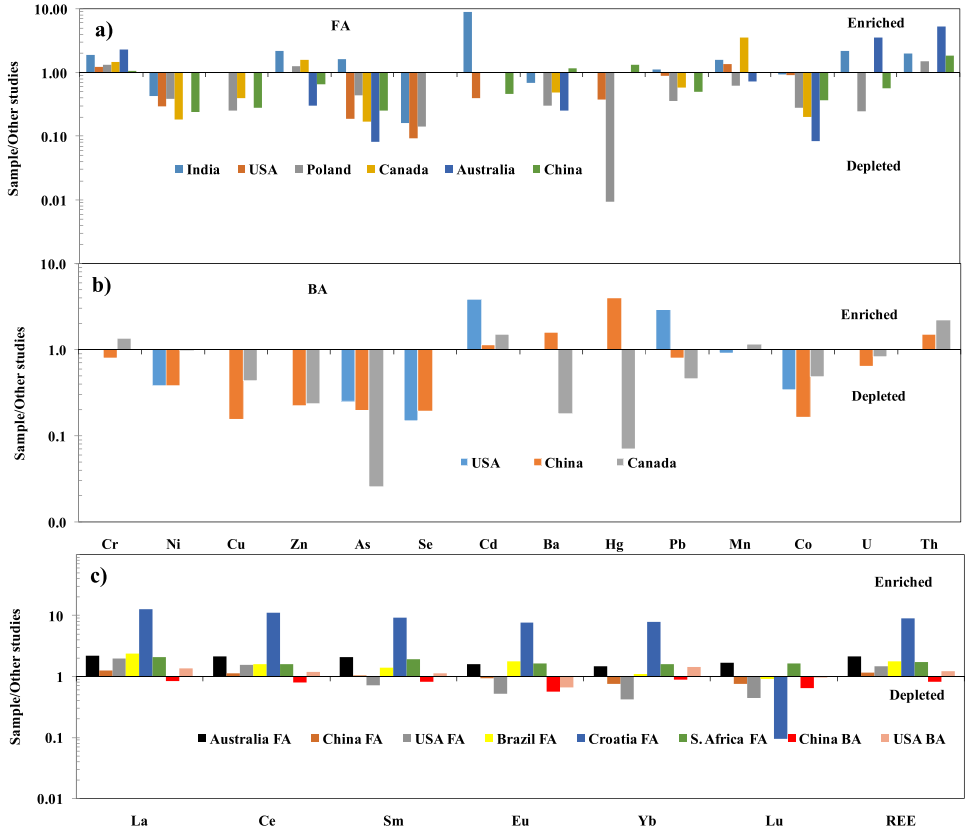

Fig. 8. Graph comparing elemental abundances in the samples with their corresponding abundances in other international studies (China: [67]; USA: [66]; (figs. a and b) [80]; (REE in FA), [22] (REE in BA); Australia: [81]; S. Africa: [28]; Canada: [109]; India: [76]; Poland: [18]; Brazil: [82]; Croatia: [12]). Plots a) and b) show toxic metals distribution, while c) individual REE elements and total REE distribution.

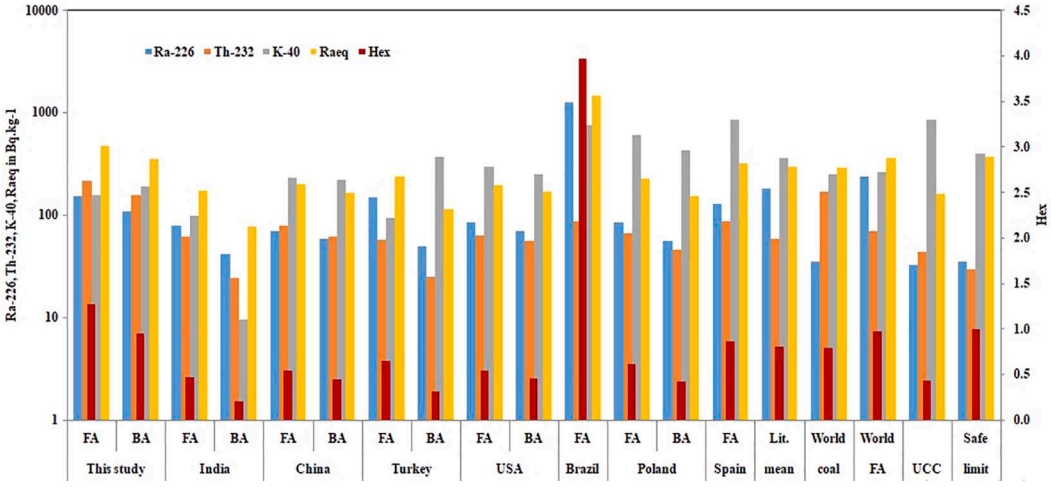

Fig. 9. Measured activity and computed radiological factors from this study mean compared with international studies and typical values for world coal and FA [85] and UCC [70]. The data is taken from the following references: Barapukuria power-station, Bangladesh (present study); India [87]; Xijiao, China [86]; Turkey [89], the USA [90]; Figueira, Brazil [91]; Lodz, Poland [92]; Spain [93]; Safe limit [85]. ^{226}Ra, ^{232}Th, ^{40}K and Radium equivalent, Ra_{eq} ($Bq.kg^{-1}$) and external hazard index, H_{ex}.

world hard coal-ash (WCA) and Upper Continental Crust (UCC) are presented in Table 2 and Fig. 7. On an average, FA contains 49.1%, 38.6%, 3.7%, 2.5%, 0.08%, 0.99%, 0.05%, and 0.89% of SiO_2, Al_2O_3, Fe_2O_3, TiO_2, MgO, CaO, Na_2O, and K_2O, respectively, while BA contains 51.0%, 34.9%, 6.7%, 2.8%, 0.81% and 1.1% of SiO_2, Al_2O_3, Fe_2O_3, TiO_2, CaO, and K_2O, respectively. The results suggest that the samples are principally composed of SiO_2, Al_2O_3, and Fe_2O_3 with minor fractions of CaO and MgO postulating Al-Si domination. The presence of Fe-oxide minerals (magnetite, hematite, Fe-spinel) in both the FA and BA residues cannot be excluded, especially since high proportions of Fe_2O_3 are occurred in the investigated samples. The obtained values (in %) for SiO_2, Al_2O_3, Fe_2O_3, TiO_2, and CaO of this study are compared with those similar studies from many countries and (e.g., China [57], India [68], Europe [69], Spain [44]) and UCC [70] represented in Table S1.

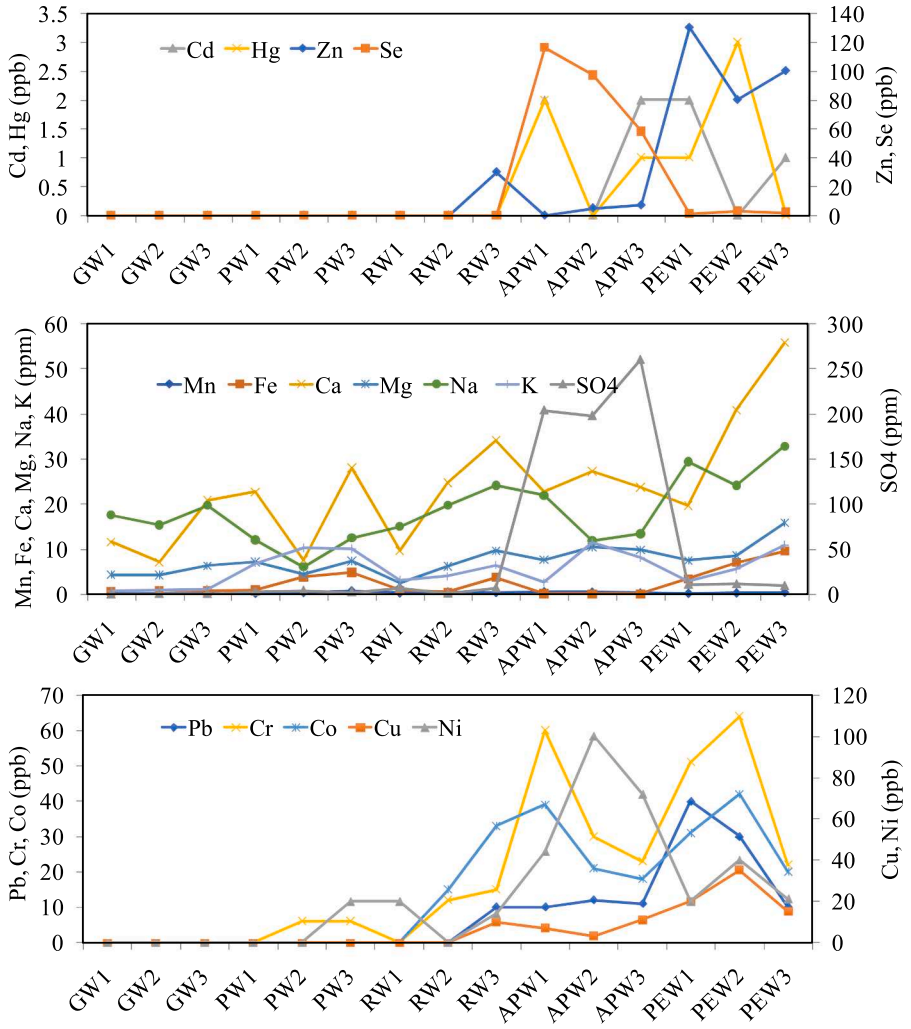

Fig. 10. Concentration of selected elements in water samples from power station surrounding, showing contrast between water ash pond and discharge water with nearby other sources. GW: groundwater; PW: pond water; RW: river water; APW: ash pond water; PEW: power-plant discharge water.

Considering the chemical composition, the studied residues are of class 'F' type and sialic type [71]. The pH of investigated FA and BA samples are 3.5 and 5.8, respectively, which demonstrate the acidic nature of the samples. In general, the sialic ash type has an overall acidic tendency and it reflects the low-CaO content of the residues [31]. Average SO_3 content in FA_{ave} is 0.67% where as in BA_{ave}, SO_3 is less than the detection limit which is eventually reflected in the lower pH of FA (Table S1). FA had a higher value of loss-on-ignition (mean: 2.2%) than BA samples (mean: 1.5%) which indicated the presence of char particles [72] in the examined samples. Among the major elements present in both alkaline and acidic residues, Ca and S (as SO_4^{2-}) are associated with more soluble phases and Al, Si, Fe and Mg are mostly partitioned in the recalcitrant phase. Elements those mainly contribute to the acidity-alkalinity of the extracts are Ca, Mg, and S, which are associated on the surface of the ash-particles [68]. The present significant Fe content detected by the XRF and SEM-EDS analyses on the particles' surfaces indicated that these particles correspond to the magnetite analyzed by XRD. This conception is in accordance with the magnetospheres containing magnetite [47]. Needles like mullite with high alumina and low silica content are found and also detected by XRD. SEM-EDS analyses indicates the presence of total C, Al, Si, K, Ca, Ti, Fe and W ranging from 0.55 to 17.7 wt% for FA and 0.47 to 23.4 wt% for BA, respectively (Table S2). Ashes with high glass contents supposed to have a low SiO_2/Al_2O_3 ratio (range: 1.2–1.5, this study). This may be originated by the crystallization of mullite during the early stages of ash generation. When mullite is separated from an initially homogeneous amorphous phase by fractional crystallization, the glass residue phase becomes enriched with SiO_2, and the quantity of glass will be declined [69]. However, in the feeding coal (bituminous) of Barapukuria, contents of SiO_2, Al_2O_3, Fe_2O_3, TiO_2, CaO, MgO, Na_2O, and K_2O were 8.1–24.3, 2.9–5.3, 3.9–5.2, 0.11–0.41, 1.7–2.7, 0.62–0.92, 0.01–0.09, and 0.26–0.75%, respectively [60–63].

3.3.2. Trace elements

Elemental distributions of the studied CCR samples are summarized in Table 2 and are compared with those in India, China, WCA, European FA, UCC and limit data [73,74] (Fig. 7b, c; 8). In general, with the few exceptions of Hf, Ni, and Ta, all the detected elements are found to be enriched in the FA_{ave} compared to those in BA_{ave} which are concomitant with Dai et al. [57] and Depoi et al. [75]. In comparison with WCA, elemental abundances of Sc, Cr, V, Mn, Ga, Zn, Cd, La, Ce, Sm, Eu, Yb, Hf, Ta, and W in FA_{ave} are slightly enriched and other elements are depleted while in the BA_{ave}, all the elements are depleted, except for Sc, Cr, Cd, La, Sm, Ce, Yb, Hf, Ta, and W (Fig. 7c). The concentrations of most of the elements in FA_{ave} are higher (by a factor of 1.1 to 5.1) as compared to Indian FA [76] and Chinese FA average [57]. The obtained values for Se, Ba, Ni, Cu, Zn, Fe, Mn, Pb, Cd, Cr, As, Hg are compared with Chinese [57], Indian [68], and European [69] FA (Fig. 8). Elements affiliated with intrinsic minerals in feeding-coal have higher volatility whereas trace-elements affiliated with extraneous minerals have lower

Table 3
Leachable concentrations (μg. L^{-1}) of selected concerned elements in the analysed ash leachates as well as their comparison with literature data and limit values (dl: below detection limit).

	Ba	As	Cd	Se	Cr	Cu	Mn	Ni	Pb	Zn	Region	Reference
This study												
FA 1	31	26	17	50	8.5	820	8200	930	23	17,100		
FA 2	180	8		20		350	1300	53	34	2200		
FA 3	170	12		80		100	980	40	18			
FA_{ave}	127.0	15.3	17.0	50.0	8.5	423.3	3493.3	341.0	25.0	9650.0	Bangladesh	This study
BA 1	640	28	1.5	16			520	20	9	50		
BA 2	210	32	2	6		190	1300	60	2	20		
BA 3	310	61		8		170	1000	80	5	40		
BA_{ave}	386.7	40.3	1.8	10.0		180.0	940.0	53.3	5.3	36.7		
Literature												
FA	1700	26	17	0	710	46	0	53	2	55	Spain	[44]
FA	3000	1100	100		2000	600	27,000	700	60	5000	Mexico	[47]
FA	193	607	1	na	na	37.3	558	79.5	23	98.3	Portugal	[31]
FA	na	85	dl	na	4	984	2180	885	126	330	India	[4]
FA	3102	633,360	1170.96	1174.2	876.9	115.72	3263.5	305.03	695.4	15345.6	Brazil	[75]
FA		3.1	11.0		5.1	14.9				82.2	China	[58]
FA	na	2.1	2.0	11.8	2.6	23.1	na	14.9	na	83.0	Australia	[64]
FA	67	6.4	0.3	0	22	450	21	69	39	810	India	[76]
FA	8.0–70.0	6.0–60.0	0–0.3	8.0–80.0	1.0–20.0	9–450	7–120	8.0–70.0	2.0–40.0	20–810	India	[76]
FA	3000–7000	<dl-20	<dl-20	20–400	1600–3400	<dl-10	–	20–100	0	30–40	China	[72,6]
FA	18–18435	10.5–12374	<dl-24	45–3661	17–9264	31–341	<dl-1200	29–513	5.0–46.0	105–724	EU	[69]
BA	na	2.4	0.1	15.1	0.4	dl	na	1.0	na	1.1	Australia	[64]
BA	na	dl	dl	na	43	680	1830	2080	44	520	India	[4]
BA	610	170	1	0	129	17	0	15	3	46	Spain	[44]
BA	4203.2	33,485	63.063	dl	99.36	65.09	1797.8	184.44	330	1413.4	Brazil	[75]
Limit values												
	0	200	200	0	100	3000	1000	2000	100	5000	India	[94]
	1500	25	5		120	750		150	50	750	China	[73]
	100,000	2000	1000	0	10,000	50,000	0	10,000	10,000	50,000	Spain	[44]
	2000	500	40	0	500	2000	0	400	500	4000	Europe	ECD, Inert [74]
	100,000	2000	1000	0	10,000	50,000	0	10,000	10,000	50,000	Europe	ECD, Non-hazardous [74]
	300,000	25,000	5000	0	70,000	100,000	0	40,000	50,000	200,000	Europe	ECD, Hazardous [74]
	700	10	3	40	50	2000	100	100	10	3000		WHO, (2011) [100]

Table 4
Contamination factor (Cf) and ecological risk factor (Er) of selected toxic and hazardous elements in the measured samples and comprehensive potential ecological risk index (RI).

	Cf		Tr[a]	Er			
	FA_{av}	BA_{av}		FA_{av}	Class	BA_{av}	Class
As	1.4	0.16	10	13.7	1	1.6	1
Cd	21.6	19.5	30	648.9	3	585.6	3
Cr	2.4	1.5	2	4.8	1	3.0	1
Cu	2.0	1.03	5	9.8	1	5.2	1
Hg	0.76	0.24	40	30.4	1	9.6	1
Mn	0.83	0.54	1	0.83	1	0.54	1
Ni	0.82	0.91	5	4.1	1	4.5	1
Pb	2.7	1.8	5	13.3	1	8.8	1
Sb	7.7	1.9	10	76.7	2	18.5	1
Zn	2.8	0.45	1	2.8	1	0.45	1
RI	–	–	–	805.3		637.7	

Tr: Biological toxic metal response factor of an individual hazardous metal.
[a] [54].

volatility [77]. From Fig. 7a, most of the elements are more enriched in the FA as compared to BA due to larger surface area of the fine particle for condensation/absorption of (semi)volatile elements which shows high affinity with these detected elements [78]. All detected elements have been found to be enriched in FA with respect to BA in exception with Fe, Ti and Zn (Fig. 7a) though, elements affiliated with clays, mica, feldspars, apatite, Fe & Ti-oxides, zircon, and other inert minerals are either slightly or non-volatile [4].

In this study, cumulative average concentrations of ∑REEs (La, Ce, Sm, Eu, Yb, and Lu, herein) are 510.3 and 359.8 ppm in the FA_{ave} and BA_{ave}, respectively, which are significantly higher than UCC (102 ppm) [70], WCA (240.8 ppm) [79], Chinese FA (183.3 ppm) and BA (209.6 ppm) [57], Chinese FA (439.5 ppm) and BA (436.3 ppm) [67], USA FA (339 ppm) [80], Raša coal ash (Croatia) (56.2 ppm) [12], Australian FA (183.3 ppm) [81], and Jorge Lacerda, Brazil (283.7 ppm) [82] (Table 2). Among the REEs contents, Ce is found to be the highest both in FA_{ave} (304.1 ppm) and BA_{ave} (218.1 ppm) samples. The measured average concentrations in ppm of this study for FA (U:12.9, Th:53.4) and for BA (U:9, Th:41.5), while Chinese FA (U:10.6, Th:37) and BA (U:10.9, Th:44.8) [57]; Chinese FA (U:22.5, Th:28.7) and BA (U:14.4, Th:28.6) [67]; Bokaro, India FA (U:7.1, Th:29.7) [76]; Australian FA (U:3.6, Th:9.9) [81]; WCA (U:15, Th:23) [79]; UCC (U:2.7, Th:10.5). Figs. 7 and 8 show major and trace elements variation for the investigated samples. The trace elements typically enriched in FA are usually more volatile elements (e.g., Mn, Ba, Co, Cr, Ni, As, Zn, Se, Pb, Hg) because they are prone to being attached to the surfaces of the ash-matrices [31]. However, the trace elemental abundances of Cr, Mn, Ni, Cd, Cu, Zn, As, Sb, Pb, Th, U, and ΣREE (La, Ce, Sm, Eu, Yb, and Lu) in feeding coals were 24.3–43.1, 48.1–57.5, 5.03–11.3, 0.7–2.7, 17.2–43.5, 13.3–33.8, 0.70–2.6, 0.38–1.6, 34.3–45.9, 9.6–13.7, 2.1–3.1, and 70.1–92.5 ppm, respectively [83,84].

3.4. Radionuclides in CCR

The mean radioactivity concentrations (in Bq.kg^{-1}) are found to be 152.2 for ^{226}Ra, 214.6 for ^{232}Th, and 158.7 for ^{40}K; and 108.7 for ^{226}Ra, 158.7 for ^{232}Th, and 190.8 for ^{40}K, in FA_{ave} and BA_{ave}, respectively (Table 2, Fig. 10). The obtained values for ^{226}Ra, ^{232}Th, and ^{40}K (in Bq. kg^{-1}) are compared with the literature data WCA (240, 70, and 265) [85]; Chinese FA (69.5, 79.3, and 233) and BA (59.5, 61.8, and 222.6) [86]; Indian FA (78.8, 61.7, and 99.1) and BA (41.4, 24.4, and 9.5) [87]; Maharashtra, India FA (110.9, 125.3 and 296.0) [88]. From the comparison, it can be observed that the measured values are significantly higher than those in world FA (except for ^{226}Ra and ^{40}K), in Indian and Chinese CCRs (except for ^{40}K in FA and BA). In Fig. 9, a summary of the measured radioactivity in the investigated samples along with international studies are shown. Measured activity concentrations of ^{226}Ra in the studied samples are significantly higher than those of the corresponding activities in the samples from India [87], China (Xijiao: [86]), Turkey [89], USA [90], Brazil (Figueira: [91]), Poland (Lodz: [92]), Spain [93], and Safe limit [85]. The determined specific activities of the samples are relatively higher compared to those of other parts of the world (e.g., Spain and India), except for Brazil.

3.5. Environmental impacts and risks assessment

3.5.1. Dispersions of potentially toxic elements

Concentrations of selected toxic elements in FA and BA leachates in comparison with other studies and limits [73,94] of industrial effluents and landfill regulations particularly those elements with known negative impacts are presented in Table 3. The extractable amounts of soluble potentially toxic elements in FA leachates are 7.7% for Se, 4.8% for Zn, and in BA 5.7% for As and 3.1% for Se and others are $< 1\%$. The mean results indicate that all considered elements are substantially released from FA during the experiment in the range of 8.5 ppb (for Cr) to 9650 ppb (for Zn) and 0.002% (for Cr) −7.7% (for Se), while from BA below detection level (for Cr) to 940 ppb (for Mn) and 0–5.7% (for As) (Table 3). In general, the measured FA samples represent relatively higher (2.1 to 22.4 times) leachability than those of BA, except for Ba and As indicating possible occurrence of the readily leachable elemental species on the surface of the FA-particles, while the most refractory portion associated in BA [4,75]. Elements on the surface of the ash-particles may release faster than those impregnated in the glassy materials, magnetite and crystalline alumosilicate phases [6,58,64]. Soluble concentrations (ppb) of potentially toxic elements follow the descending order as Zn > Mn > Cu > Ni > Ba > Se > Pb > Cd > As > Cr, and in percentage of leachability Mn > Ba > Cu > Ni > As > Zn > Se > Pb > Cd > Cr released from FA whereas, Se > Zn > Cu > Ni > Mn > As > Cd > Pb > Ba > Cr and As > Se > Cu > Mn > Zn > Ni > Cd > Ba > Pb > Cr from BA, respectively and postulate good accordance with other valuable works [36,76]. While both TCLP and water-based leaching tests carried out on acidic-generating Australian FA removed 0.3–20% of As, a significant difference between water leaching (0.3–15%) was noted. The mobility characteristically varied between 0.02 and 2% for Ba [95]. Water extractable fractions for a suite of 23 EU residues were in the 0.001–25% range [69], 3–9% Cd was extracted at a pH of 4 from acidic-natured Australian FA [96]. Leaching tests on acidic FA from Australia hardly mobilized any Cr (0.03%) [97], Pb was found to be highly insoluble and almost immobile in both alkaline and acidic-natured FA, irrespective of the pH and the leaching test [27,69]. As with other cations, acidic conditions slightly augment the Pb leaching [98] while Zn is 3–9% extractable at pH≈1–2 [99]. These findings highlight a possibility of contamination from presently investigated CCRs. However, Hg has also been checked but not detected due to its very low abundance. The detected elements in FA may mobilize into the environment when improperly dumped and might cause significant environmental consequences [31]. The released concentration of some individual elements in FA exceeded the other studies (Table 3) but still far below than the European prescribed inert limit [74] for respective species, with the exception only for Zn and though, the total concentrations of Zn, Ni, Se, Pb, Cd, As, and Mn significantly exceed the WHO guideline [100], might be considered as non-hazardous-inert landfill materials according to the European Council Decision 2003/33/EC. Hence, the disposal of discussed residues should be handled carefully and monitored to keep away from the probable pollution in the plant proximity.

3.5.2. Impacts on water resources

The effect of the leaching characteristics from the residue was evaluated in this research in the ash-ponds water, routine effluents discharge and other proximal water sources in the vicinity of the power-station, which is presented in Fig. 10. The levels of elements in water at the intake, from where plant receives its cooling water and effluent discharge points of the power-station exhibit significant inconsistence. The occurrence of potentially toxic elements is in the water discharged from the plant while those are not detected the intake samples (Fig. 10) indicating contribution of CCRs to effluent water. The CCR are possibly the prime source to significantly increase the content of chemical species present in the discharged water, as was reflected in the increased SO_4^{2-} content to the plant intake water which is presumably derived from CCRs. In this regard, it is important to note that the water received by the power plant is de-mineralized before utilization. In sum therefore, there is an addition of elements in the water taken up by the plant, which included also the way they discharge the effluents, from the treatment plant into the ash-ponds where certain elements could be released and then channeled into the nearby river (Tilai). There is a certain possibility to release, leak, and migrate of those well-known elements from non-lined ash pond resulting to contaminate most essential and invaluable groundwater bearing aquifer. The observed results of this study exceeded the respective limits for drinking water [101]. While low levels of elements in the groundwater source are detected in the area while increased concentrations of those are found in analyzed ash-ponds water, effluents draining to nearby river and presumable leached, migrate and percolate to groundwater from the ash-ponds and other temporary ash storage sites and exceeding their corresponding limit values.

The concentrations (average; range) (ppb) of As (48.9; 0–232.0), Cd (0.47; 0–2.0), Co (14.6; 0–42.0), Cr (19.3; 0–64.0), Cu (6.7; 0–35.0), Mn (280; 80–670), Ni (23.4; 0–100.0), Pb (8.2; 0–40.0), Se (18.5; 0–116.0), Hg (0.47; 0–3.0), and Zn (23.5; 0–130.0) and others in ppm Fe (2.5; 0.1–9.5), Ca (23.7; 7.1–55.7), Mg (7.4; 2.4–15.8), Na (18.3;6.1–32.8), K (5.7; 0.72–11.5), and SO_4^{2-} (47.8; 0–260.0) in waters from different sources nearby power-station (Fig. 10) were obtained in this study. The concern is about elevated SO_4^{2-} in samples in the downstream of the ash-pond [102]. Significantly high concentrations of Se and As in ash-ponds water and effluent discharge water are obviously being contributed from ash-particles. Surprisingly those are not detected in CCR containing elements are being inappropriately disposed of to the nearby unlined ash-ponds thereby these materials tend to be leached, weathered, migrate and exposed to nearby water sources and elevate the background concentration of those elements. This contaminated water would ultimately runoff, percolate and migrate to the ambient environmental systems. Opened stackable residues at power-station premise are blown and carried by runoff due to raining as well as commonly mixed with internal surface drainages of the power-station and simultaneously release those elements in the water sources and subsequently transport to the adjacent Tilai River and other water systems and modify the background composition thereby.

In Bangladesh, remarkable increased concentrations of Mn, Fe, Cu, Zn, and Cr [103]; Cr, As, Cd, Mn and Fe [104]; Pb, Cd and Cr [35] are determined in water sources in the vicinity of the plant. In India, As, Zn, Ba, Se and Pb [105]; As [106]; in USA As, Se, Cr and Ba [107]; in Greece Cr, Mn, Ni, Cu, Zn, and Pb [36] show relatively higher concentrations in the water systems closest to ash-ponds to nearby water sources, indicating significant input from CCRs source and ash spill event and

exceeded admissible levels proposed by WHO [100]. And also similar cases have also been reported by others [14,108] India (Andhra Pradesh and Maharashtra) leaching of As and Se from FA samples can moderately affect water systems [46]. It is a matter of concern in terms of leachability of certain toxic elements in CCRs. These may be mobilized into the environment if waste materials are improperly dumped, may leach and migrate to water systems causing adverse environmental consequences and endanger human health [9,31,32,36,37].The content of these elements in studied samples may have unusual adverse impacts on the environment, fisheries and other water lives under favorable conditions. Due to their bioavailability (bio-accessibility), bio-reactivity, toxicity, carcinogenicity, and mutagenicity effects could pose deleterious and long-lasting environmental problems even at low levels [23,109–112]. Upon exposure, concerned elements (e.g., Pb, Cr, Cd, Hg, Ni, As) can be accumulated in human body and interact with proteins and finally could damage almost every organ, notably the kidneys and heart [113], nervous systems, lung tumors, liver failure, etc. Moreover, high exposure levels of REEs are likely related to health problems such as liver function decline [39,40].

3.5.3. Ecological and radiological risks

The estimated Er^{i} values are below 40, and they posed a 'low potential ecological risk' to the environment for all considered toxic elements, except for Cd (648.9 for FA and 585.6 for BA representing very high risk). For all considered elements, comprehensive RI estimation is found to be 'very high' risk to the environment for FA_{ave} (805.3) and BA_{ave} (637.7) (Table 4) which is consistent with the findings of Pandey and Bhattacharya [55]. The RI values suggest moderate risk from FA and low risk from BA to the environment, according to the threshold values. On the other hand, the mean values of radiological hazard indices in the CCRs are 471.4 $Bq.kg^{-1}$(FA) and 350.4 $Bq.kg^{-1}$(BA) for Ra_{eq}; 1.27 and 0.95 for H_{ex}, respectively, indicating a potential risk of ionizing radiation exposure. The values for analyzed FA exceed the permissible limit, suggesting a potential radiological threat to the environment as well as to the human health of BCPP nearby inhabitants [6,33].

4. Conclusion

Depending on the experimental data and their associated assessment, the following conclusions can be drawn:

1. The CCR are mainly comprised of glassy-matrix (94.8%), crystalline phases (3.6%), anisotropic-coke and slightly altered inertinite (1.3%), and partially baked rock-fragments (0.3%). Residual spinel, hematite, magnetite, mullite, quartz, and cristobalite comprise the major crystallite phases whereas monazite, zircon, rutile, tourmaline, and sillimanite are identified in the accessory phases.
2. All detectable elements (Al, Sc, V, Cr, Mn, Co, Ni, Cu, Zn, Ga, As, Br, Rb, Cd, Sb, Cs, Ba, La, Ce, Sm, Eu, Yb, Lu, Hf, Ta, W, Hg, Pb, Th, and U) are found to be enriched (by a factor of 1.2 to 14.2) in the FA and BA, as compared to PC, except for Ni in the FA; and Zn, As, Cu, and Hg in the BA. In comparison with the WCA, the obtained contents for Mn, Th, and Cd in the CCR are slightly enriched, while others are depleted. Cumulative average concentrations (in ppm) of REEs (here La, Ce, Sm, Eu, Yb, and Lu) are 510.3 in the FA and 359.8 in the BA, which are significantly higher than the WCA average (240.8). The SEM-EDS analysis demonstrated that the dominant surface compositions of spheres are C, Al and Si with minor K, Ca, Mg, Ti, Fe, and W.
3. The specific activity of the CCR are considerably higher by a factor of 3.7 (^{226}Ra) to 6.2 (^{232}Th) than those of the WC average. In addition, CCR of this study possess higher level of activity typically ^{232}Th by a factor of 2.7 to 6.2 as compare to the WCA. Radiation hazard indices including radium equivalent activity (Ra_{eq}) and external hazard index (H_{ex}) exceed the permissible limits for FA.
4. Along with the environmental and ecological indices, a preliminary assessment of some specific element's dispersion to the environment has also been performed through leaching test which reveals that lime contents and pH likely control the elemental leaching.
5. Qualitative measurements confirm the presence of contaminants in studied CCR, which may cause several acute health risks and impact on environment. Monitoring the surrounding water resources and CCR-leachates along with the indices-based ecological risk estimation reveal the adverse environmental impacts of CCRs.

The outcome of this study reveals the comprehensive characteristics of the coal combustion residues from a coal-based power plant for the first time where feed coal is sourced from the Barapukuria, Bangladesh. Inherent properties of CCRs and their associated potential adverse impacts on environment human health are evaluated. The findings of this work will provide a regional baseline data for the CCRs which can be utilized in the identical cases around the world.

CRediT authorship contribution statement

Abdul Baquee Khan Majlis: Investigation, Data curation. **Md. Ahosan Habib:** Conceptualization, Methodology, Writing – original draft. **Rahat Khan:** Conceptualization, Validation, Writing – review & editing. **Khamphe Phoungthong:** Data curation, Validation. **Kuaanan Techato:** Supervision, Conceptualization, Writing – review & editing. **Md Aminul Islam:** Writing – review & editing. **Satoru Nakashima:** Data curation, Validation. **Abu Reza Md. Towfiqul Islam:** Visualization. **Madison M. Hood:** Data curation. **James C. Hower:** Writing – review & editing.

Declaration of Competing Interest

The authors declare that they have no known competing financial interests or personal relationships that could have appeared to influence the work reported in this paper.

Acknowledgements

This research was supported by Prince of Songkla University under the Postdoctoral Fellowship Program. The authority of the Geological Survey of Bangladesh deserves appreciation for official support to carry out this research. The authority of Barapukuria Power-plant is greatly acknowledged for giving permission and providing the necessary samples for this research. Authors are also deeply thankful to Alam Surya Wijaya, Md. Rubel Sheik for their kind assistance and cooperation during conducting this research.

Appendix A. Supplementary data

Supplementary data to this article can be found online at https://doi.org/10.1016/j.fuel.2022.124711.

References

[1] Swanson SM, Engle MA, Ruppert LF, Affolter RH, Jones KB. Partitioning of selected trace elements in coal combustion products from two coal-burning power plants in the United States. Int J Coal Geol 2013;113:116–26. https://doi.org/10.1016/j.coal.2012.08.010.
[2] Hower JC, Fu B, Dai S. Geochemical partitioning from pulverized coal to fly ash and bottom ash. Fuel 2020;279(June). https://doi.org/10.1016/j.fuel.2020.118542.
[3] Habib MA, Khan R. Environmental Impacts of Coal-Mining and Coal-Fired Power-Plant Activities in a Developing Country with Global Context (chapter 24). In: Shit P.K., Adhikary P.P., Sengupta D. (eds.) *Spatial Modeling and Assessment of Environmental Contaminants* 2021;421-493. Environmental Challenges and Solutions. Springer, Cham.
[4] Verma SK, Masto RE, Gautam S, Choudhury DP, Ram LC, Maiti SK, et al. Investigations on PAHs and trace elements in coal and its combustion residues from a power plant. Fuel 2015;162:138–47. https://doi.org/10.1016/j.fuel.2015.09.005.
[5] Xie J, Niu XD, He KQ, He KQ, Shi MD, Yu SJ, et al. Arsenic and selenium distribution and speciation in coal and coal combustion by-products from coal-

fired power plants. Fuel 2021;292(February):120228. https://doi.org/10.1016/j.fuel.2021.120228.
[6] Li J, Zhuang X, Querol X, Font O, Moreno N. A review on the applications of coal combustion products in China. Int Geol Rev 2018;60(5–6):671–716. https://doi.org/10.1080/00206814.2017.
[7] Silva LFO, DaBoit K, Sampaio CH, Jasper A, Andrade ML, Kostova IJ, et al. The occurrence of hazardous volatile elements and nanoparticles in Bulgarian coal fly ashes and the effect on human health exposure. Sci Total Environ 2012;416:513–26.
[8] Ruhl L, Vengosh A, Dwyer GS, Hsu-Kim H, Deonarine A, Bergin M, et al. Survey of the potential environmental and health impacts in the immediate aftermath of the coal ash spill in Kingston, Tennessee. Environ Sci Technol 2009;43(16):6326–33.
[9] Saikia BK, Saikia J, Rabha S, Silva LFO, Finkelman R. Ambient nanoparticles/nanominerals and hazardous elements from coal combustion activity: Implications on energy challenges and health hazards. Geosci Front 2018;9(3):863–75. https://doi.org/10.1016/j.gsf.2017.11.013.
[10] Wang N, Sun X, Zhao Q, Yang Y, Wang P. Leachability and adverse effects of coal fly ash: A review. J Hazard Mater 2020;396(January). https://doi.org/10.1016/j.jhazmat.2020.122725.
[11] Meawad AS, Bojinova DY, Pelovski YG. An overview of metals recovery from thermal power plant solid wastes. Waste Manag 2010;30(12):2548–59. https://doi.org/10.1016/j.wasman.2010.07.010.
[12] Fiket Ž, Medunić G, Furdek Turk M, Kniewald G. Rare earth elements in superhigh-organic-sulfur Raša coal ash (Croatia). Int J Coal Geol 2018;194(May):1–10. https://doi.org/10.1016/j.coal.2018.05.002.
[13] Wagner NJ, Matiane A. Rare earth elements in select Main Karoo Basin (South Africa) coal and coal ash samples. Int J Coal Geol 2018;196(February):82–92. https://doi.org/10.1016/j.coal.2018.06.020.
[14] Vengosh A, Cowan EA, Coyte RM, Kondash AJ, Wang Z, Brandt JE, et al. Evidence for unmonitored coal ash spills in Sutton Lake, North Carolina: Implications for contamination of lake ecosystems. Sci Total Environ 2019;686:1090–103.
[15] Habib MA, Khan R, Phoungthong K. Evaluation of environmental radioactivity in soils around a coal burning power plant and a coal mining area in Barapukuria, Bangladesh: Radiological risks assessment. Chem. Geol. 2022;600:120865. https://doi.org/10.1016/j.chemgeo.2022.120865.
[16] Vejahati F, Xu Z, Gupta R. Trace elements in coal : Associations with coal and minerals and their behavior during coal utilization – A review. Fuel 2010;89(4):904–11. https://doi.org/10.1016/j.fuel.2009.06.013.
[17] Izquierdo M, Querol X. Leaching behaviour of elements from coal combustion fly ash: An overview. Int J Coal Geol 2012;94:54–66. https://doi.org/10.1016/j.coal.2011.10.006.
[18] Lanzerstorfer C. Fly ash from coal combustion: Dependence of the concentration of various elements on the particle size. Fuel May 2017;2018(228):263–71. https://doi.org/10.1016/j.fuel.2018.04.136.
[19] Yao ZT, Ji XS, Sarker PK, Tang JH, Ge LQ, Xia MS, et al. A comprehensive review on the applications of coal fly ash. Earth-Sci Rev 2015;141:105–21.
[20] Hower JC, Groppo JG, Graham UM, Ward CR, Kostova IJ, Maroto-Valer MM, et al. Coal-derived unburned carbons in fly ash: A review. Int J Coal Geol 2017;179(May):11–27. https://doi.org/10.1016/j.coal.2017.05.007.
[21] Hower JC, Henke KR, Dai S, Ward CR, French D, Liu S, et al. *Generation and Nature of Coal Fly Ash and Bottom Ash*. Chapter 2 (21–65). In: Robl T, Oberlink A, Jones R, editors. Coal Combustion Products (CCP's): Characteristics, Utilization and Beneficiation. Duxford, United Kingdom: Woodhead Publishing, an imprint of Elsevier; 2017. https://doi.org/10.1016/B978-0-08-100945-1.00002-2.
[22] Hower JC, Groppo JG, Henke KR, Graham UM, Hood MM, Joshi P, et al. Ponded and Landfilled Fly Ash as a Source of Rare Earth Elements from a Kentucky Power Plant. Coal Combust Gasif Prod 2017;9(1):1–21. https://doi.org/10.4177/ccgp-d-17-00003.1.
[23] Saikia BK, Hower JC, Hood MM, Baruah R, Dekaboruah HP, Boruah R, et al. Petrological and biological studies on some fly and bottom ashes collected at different times from an Indian coal-based captive power plant. Fuel 2015;158:572–81.
[24] Parzentny HR, Róg L. Distribution and mode of occurrence of Co, Ni, Cu, Zn, As, Ag, Cd, Sb, Pb in the feed coal, fly ash, slag, in the topsoil and in the roots of trees and undergrowth downwind of three power stations in poland. Minerals 2021;11(2):1–33. https://doi.org/10.3390/min11020133.
[25] Gollakota ARK, Volli V, Shu CM. Progressive utilisation prospects of coal fly ash: A review. Sci Total Environ 2019;672:951–89. https://doi.org/10.1016/j.scitotenv.2019.03.337.
[26] Zierold KM, Odoh C. A review on fly ash from coal-fired power plants: Chemical composition, regulations, and health evidence. Rev Environ Health 2020;35(4):401–18. https://doi.org/10.1515/reveh-2019-0039.
[27] Praharaj T, Powell MA, Hart BR, Tripathy S. Leachability of elements from sub-bituminous coal fly ash from India. Environ Int 2002;27(8):609–15.
[28] Eze CP, Fatoba O, Madzivire G, Ostrovnaya TM, Petrik LF, Frontasyeva MV, et al. Elemental composition of fly ash: a comparative study using nuclear and related analytical techniques. Chem Didact Ecol Metrol 2013;18(1–2):19–29.
[29] Tian HZ, Lu L, Hao JM, Gao JJ, Cheng K, Liu KY, et al. A review of key hazardous trace elements in chinese coals: Abundance, occurrence, behavior during coal combustion and their environmental impacts. Energy Fuels 2013;27(2):601–14.
[30] Oliveira MLS, Marostega F, Taffarel SR, Saikia BK, Waanders FB, DaBoit K, et al. Nano-mineralogical investigation of coal and fly ashes from coal-based captive power plant (India): An introduction of occupational health hazards. Sci Total Environ 2014;468-469:1128–37.
[31] Ribeiro J, Valentim B, Ward C, Flores D. Comprehensive characterization of anthracite fly ash from a thermo-electric power plant and its potential environmental impact. Int J Coal Geol 2011;86(2–3):204–12. https://doi.org/10.1016/j.coal.2011.01.010.
[32] Habib MA, Basuki T, Miyashita S, Bekelesi W, Nakashima S, Techato K, et al. Assessment of natural radioactivity in coals and coal combustion residues from a coal-based thermoelectric plant in Bangladesh: Implications for radiological health hazards. Environ Monit Assess 2019;191(2). https://doi.org/10.1007/s10661-019-7233-6.
[33] Habib MA, Basuki T, Miyashita S, Bekelesi W, Nakashima S, Phoungthong K, et al. Distribution of naturally occurring radionuclides in soil around a coal-based power plant and their potential radiological risk assessment. Radiochim Acta. 2019;107(3):243-259. doi:10.1515/ract-2018-3044.
[34] Habib MA, Islam ARMT, Bodrud-Doza Md, Mukta FA, Khan R, Bakar Siddique MA, et al. Simultaneous appraisals of pathway and probable health risk associated with trace metals contamination in groundwater from Barapukuria coal basin, Bangladesh. Chemosphere 2020;242:125183.
[35] Karamanis D, Ioannides K, Stamoulis K. Environmental assessment of natural radionuclides and heavy metals in waters discharged from a lignite-fired power plant. Fuel 2009;88(10):2046–52. https://doi.org/10.1016/j.fuel.2009.02.032.
[36] Zhao L, Dai S, Finkelman RB, French D, Graham IT, Yang Y, et al. Leaching behavior of trace elements from fly ashes of five Chinese coal power plants. Int J Coal Geol 2020;219(November 2019):103381. doi:10.1016/j.coal.2019.103381.
[37] Saikia BK, Hower JC, Islam N, Sharma A, Das P. Geochemistry and petrology of coal and coal fly ash from a thermal power plant in India. Fuel 2021;291(January):120122. https://doi.org/10.1016/j.fuel.2020.120122.
[38] Hower JC. Petrographic examination of coal-combustion fly ash. Int J Coal Geol 2012;92:90–7. https://doi.org/10.1016/j.coal.2011.12.012.
[39] Khan R, Parvez MS, Jolly YN, Haydar MA, Alam MF, Khatun MA, et al. Elemental abundances, natural radioactivity and physicochemical records of a southern part of Bangladesh: Implication for assessing the environmental geochemistry. Environ Nanotechnol Monit Manag 2019;12(February):100225. doi:10.1016/j.enmm.2019.100225.
[40] Khan R, Islam HMT, Islam ARMT. Mechanism of elevated radioactivity in Teesta river basin from Bangladesh: Radiochemical characterization, provenance and associated hazards. Chemosphere 2021;264:128459.
[41] Khan R, Mohanty S, Sengupta D. Studying the elemental distribution in the core sediments of Podampata, Eastern coast of Odisha, India: Potentiality of rare earth elements and Th exploration. Arab J Geosci 2021;14:81. doi:10.1007/s12517-020-06371-x.
[42] Khan R, Islam HMT, Apon MAS, Islam, ARMT, Habib MA, Phoungthong K, et al. Environmental geochemistry of higher radioactivity in a transboundary Himalayan River sediment (Brahmaputra, Bangladesh): Potential radiation exposure and health risks. Environ Sci Pollut Res 2022: (in press). doi:10.1007/s11356-022-19735-5.
[43] Tamim U, Khan R, Jolly YN, Fatema K, Das S, Naher K, et al. Elemental distribution of metals in urban river sediments near an industrial effluent source. Chemosphere 2016;155:509–18.
[44] Álvarez-Ayuso E, Querol X, Tomás A. Environmental impact of a coal combustion-desulphurisation plant: Abatement capacity of desulphurisation process and environmental characterisation of combustion by-products. Chemosphere 2006;65(11):2009–17. https://doi.org/10.1016/j.chemosphere.2006.06.070.
[45] American Society for Testing and Materials (ASTM D6357-2011). Test Methods for Determination of Trace Elements in Coal, Coke, and Combustion Residues from Coal Utilization Processes by Inductively Coupled Plasma Atomic Emission, Inductively Coupled Plasma Mass, and Graphite Furnace Atomic Absorption Spectrometry. In ASTM, PA, USA; 2011.
[46] Sandeep P, Sahu SK, Kothai P, Pandit GG. Leaching Behavior of Selected Trace and Toxic Metals in Coal Fly Ash Samples Collected from Two Thermal Power Plants, India. Bull Environ Contam Toxicol 2016;97(3):425–31. https://doi.org/10.1007/s00128-016-1864-x.
[47] Medina A, Gamero P, Querol X, Moreno N, De León B, Almanza M, et al. Fly ash from a Mexican mineral coal I: Mineralogical and chemical characterization. J Hazard Mater 2010;181(1-3):82–90.
[48] Phoungthong K, Xia Y, Zhang H, Shao L, He P. Leaching toxicity characteristics of municipal solid waste incineration bottom ash. Front Environ Sci Eng 2016;10(2):399–411. https://doi.org/10.1007/s11783-015-0819-5.
[49] Hossain S, Anik AH, Khan R, Ahmed FT, Siddique MAB, Khan AH, et al. Public health vulnerability due to the exposure of dissolved metal(oid)s in tap water from a mega city (Dhaka, Bangladesh): Source and quality appraisals. Expos Health 2022. https://doi.org/10.1007/s12403-021-00446-0.
[50] Rahman MA, Siddique MAB, Khan R, Reza AHMS, Khan AH, Akbor MA, et al. Mechanism of arsenic enrichment and mobilization in groundwater from southeastern Bangladesh: Water quality and preliminary health risks assessment. Chemosphere 2022. https://doi.org/10.1016/j.chemosphere.2022.133556.
[51] American Public Health Association. In: Baird, R.B., Eaton, A.D., Rice, E. W. (Eds.), Standard Methods for the Examination of Water and Wastewater, 23th ed., American Water Works Association, Water Environment Federation, Washington, DC, USA; 2017.
[52] Ahsan MA, Satter F, Siddique MAB, Akbor MA, Ahmed S, Shajahan M, et al. Chemical and physicochemical characterization of effluents from the tanning and textile industries in Bangladesh with multivariate statistical approach. Environ Monit Assess 2019;191:575. https://doi.org/10.1007/s10661-019-7654-2.
[53] Islam ARMT, Islam HMT, Mia MU, Khan R, Habib MA, Bodrud-Doza M, et al. Co-distribution, possible origins, status and potential health risk of trace elements in

surface water sources from six major river basins, Bangladesh. Chemosphere 2020;249:126180. https://doi.org/10.1016/j.chemosphere.2020.126180.
[54] Hakanson L. An ecological risk index for aquatic pollution control. A sedimentological approach. Water Res 1980;14(8):975–1001.
[55] Pandey SK, Bhattacharya T. Mobility, Ecological risk and change in surface morphology during sequential chemical extraction of heavy metals in fly ash: A case study. Environ Technol Inno 2019;13:373–82.
[56] Levandowski J, Kalkreuth W. Chemical and petrographical characterization of feed coal, fly ash and bottom ash from the Figueira Power Plant, Paraná, Brazil. Int J Coal Geol 2009;77(3–4):269–81. https://doi.org/10.1016/j.coal.2008.05.005.
[57] Dai S, Zhao L, Hower JC, Johnston MN, Song W, Wang P, et al. Petrology, mineralogy, and chemistry of size-fractioned fly ash from the Jungar power plant, Inner Mongolia, China, with emphasis on the distribution of rare earth elements. Energy Fuels 2014;28(2):1502–14.
[58] Fu B, Liu G, Mian MM, Sun M, Wu D. Characteristics and speciation of heavy metals in fly ash and FGD gypsum from Chinese coal-fired power plants. Fuel 2019;251(April):593–602. https://doi.org/10.1016/j.fuel.2019.04.055.
[59] Bartoňová L. Unburned carbon from coal combustion ash: An overview. Fuel Process Technol 2015;134:136–58. https://doi.org/10.1016/j.fuproc.2015.01.028.
[60] Bakr MA, Rahman QMA, Islam MM, Islam MK, Uddin MN, Resan SA, et al. Geology and coal deposit of Barapukuria Basin, Dinajpur district, Bangladesh. Records of the Geological Survey of Bangladesh, Government publication. Bangladesh 1996;8(1).
[61] Farhaduzzaman M, Abdullah WH, Islam MA. Depositional environment and hydrocarbon source potential of the Permian Gondwana coals from the Barapukuria Basin, Northwest Bangladesh. Int J Coal Geol 2016;2012(90–91):162–79. https://doi.org/10.1016/j.coal.2011.12.006.
[62] Farhaduzzaman M, Abdullah WH, Islam MA. Petrographic characteristics and palaeoenvironment of the Permian coal resources of the Barapukuria and Dighipara basins, Bangladesh. J Asian Earth Sci 2013;64:272–87. https://doi.org/10.1016/j.jseaes.2012.12.017.
[63] Farhaduzzaman M, Abdullah WH, Islam MA, Pearson MJ. Organic facies variations and hydrocarbon generation potential of Permian Gondwana group coals and associated sediments, Barapukuria and Dighipara basins, NW Bangladesh. J Pet Geol 2013;36(2):117–37. https://doi.org/10.1111/jpg.12547.
[64] Ward CR, French D, Jankowski J, Dubikova M, Li Z, Riley KW. Element mobility from fresh and long-stored acidic fly ashes associated with an Australian power station. Int J Coal Geol 2009;80(3–4):224–36. https://doi.org/10.1016/j.coal.2009.09.001.
[65] Vassilev SV, Vassileva CG, Karayigit AI, Bulut Y, Alastuey A, Querol X. Phase-mineral and chemical composition of composite samples from feed coals, bottom ashes and fly ashes at the Soma power station, Turkey. Int J Coal Geol 2005;61(1–2):35–63. https://doi.org/10.1016/j.coal.2004.06.004.
[66] Demir I, Hughes RE, DeMaris PJ. Formation and use of coal combustion residues from three types of power plants burning Illinois coals. Fuel 2001;80(11):1659–73. https://doi.org/10.1016/S0016-2361(01)00028-X.
[67] Wang Z, Dai S, Zou J, French D, Graham IT. Rare earth elements and yttrium in coal ash from the Luzhou power plant in Sichuan, Southwest China: Concentration, characterization and optimized extraction. Int J Coal Geol 2018;2019(203):1–14. https://doi.org/10.1016/j.coal.2019.01.001.
[68] Ram LC, Masto RE. Fly ash for soil amelioration : A review on the in fl uence of ash blending with inorganic and organic amendments. Earth Sci Rev 2014;128:52–74. https://doi.org/10.1016/j.earscirev.2013.10.003.
[69] Moreno N, Querol X, Andrés JM, Stanton K, Towler M, Nugteren H, et al. Physico-chemical characteristics of European pulverized coal combustion fly ashes. Fuel 2005;84(11):1351–63. https://doi.org/10.1016/j.fuel.2004.06.038.
[70] Rudnick RL, Gao S. Composition of the continental crust, Chapter 4 (1–64). In: Holland HD, Turekian KK, editors. Treatise on Geochemistry. 2nd ed. Amsterdam, Netherlands; Oxford, England; Waltham, Massachusetts: Elsevier; 2014.
[71] Vassilev SV, Vassileva CG. A new approach for the classification of coal fly ashes based on their origin, composition, properties, and behaviour. Fuel 2007;86(10–11):1490–512. https://doi.org/10.1016/j.fuel.2006.11.020.
[72] Li J, Zhuang X, Querol X, Font O, Moreno N, Zhou J. Environmental geochemistry of the feed coals and their combustion by-products from two coal-fired power plants in Xinjiang Province, Northwest China. Fuel 2012;95:446–56. https://doi.org/10.1016/j.fuel.2011.10.025.
[73] GB 18598. Standard for pollution control on the security landfill site for hazardous wastes: Beijing, National Chinese Standard, Ministry of Environmental Protection of the People's Republic of China; 2001.
[74] European Council Decision (ECD). Decision, 2003/33/EC of 19 December 2002 establishing criteria and procedures for the acceptance of waste at landfills pursuant to Article 16 of and Annex II to Directive 1999/31/EC, Official Journal of the European Union 11, 2003; 27–49.
[75] Depoi FS, Pozebon D, Kalkreuth WD. Chemical characterization of feed coals and combustion-by-products from Brazilian power plants. Int J Coal Geol 2008;76(3):227–36. https://doi.org/10.1016/j.coal.2008.07.013.
[76] Shreya N, Valentim B, Paul B, Guedes A, Pinho S, Ribeiro J, et al. Multi-technique study of fly ash from the Bokaro and Jharia coalfields (Jharkhand state, India): A contribution to its use as a geoliner. Int J Coal Geol 2015;152:25–38.
[77] Querol X, Fernández-Turiel J, López-Soler A. Trace elements in coal and their behaviour during combustion in a large power station. Fuel 1995;74(3):331–43.
[78] Dai S, Zhao L, Peng S, Chou C-L, Wang X, Zhang Y, et al. Abundances and distribution of minerals and elements in high-alumina coal fly ash from the Jungar Power Plant, Inner Mongolia, China. Int J Coal Geol 2010;81(4):320–32.
[79] Ketris MP, Yudovich YE. Estimations of Clarkes for Carbonaceous biolithes: World averages for trace element contents in black shales and coals. Int J Coal Geol 2009;78(2):135–48. https://doi.org/10.1016/j.coal.2009.01.002.
[80] Hower J, Groppo J, Henke K, Hood M, Eble C, Honaker R, et al. Notes on the potential for the concentration of rare earth elements and yttrium in coal combustion fly ash. Minerals 2015;5(2):356–66.
[81] Fardy J, McOrist G, Farrar Y. Neutron activation analysis and radioactivity measurements of Australian coals and fly ashes. J Radioanal Nucl Chem 1989;133(2):217–26.
[82] Silva L, Ward C, Hower J, Izquierdo M, Waanders F, Oliveira M, et al. Mineralogy and Leaching Characteristics of Coal Ash from a Major Brazilian Power Plant. Coal Combust Gasif Prod 2010;2(1):51–65.
[83] Islam MA, Latif SA, Hossain SM, Uddin MS, Podder J. The concentration and distribution of trace elements in coals and ashes of the Barapukuria thermal power plant, Bangladesh. Energy Sour Part A 2011;33(5):392–400. https://doi.org/10.1080/15567030903030708.
[84] Podder J, Tarek SA, Hossain T. Trace Elemental Analysis of Permian Gondwana Coals in Bangladesh By Pixe Technique. Int J PIXE 2004;14:89–97. https://doi.org/10.1142/s0129083504000148.
[85] United Nations Scientific Committee on the Effects of Atomic Radiation (UNSCEAR). Sources and effects of ionizing radiation. Report to the General Assembly, with Scientific Annexes. United Nations (A/55/46), New York; 2000.
[86] Lu X, Li LY, Wang F, Wang L, Zhang X. Radiological hazards of coal and ash samples collected from Xi'an coal-fired power plants of China. Environ Earth Sci 2012;66(7):1925–32. https://doi.org/10.1007/s12665-011-1417-x.
[87] Sahu SK, Tiwari M, Bhangare RC, Pandit GG. Enrichment and particle size dependence of polonium and other naturally occurring radionuclides in coal ash. J Environ Radio 2014;138:421–6.
[88] Voltaggio M, Spadoni M, Sacchi E, Sanam R, Pujari PR, Labhasetwar PK. Assessment of groundwater pollution from ash ponds using stable and unstable isotopes around the Koradi and Khaperkheda thermal power plants (Maharashtra, India). Sci Total Environ 2015;518:616–25.
[89] Cevik U, Damla N, Koz B, Kaya S. Radiological characterization around the Afsin-Elbistan coal-fired power plant in Turkey. Energy Fuels 2008;22(1):428–32.
[90] Coles DG, Ragaini RC, Ondov JM. Behavior of natural radionuclides in western coal-fired power plants. Environ Sci Technol 1978;12(4):442–6.
[91] Flues M, Camargo IMC, Silva PSC, Mazzilli BP. Radioactivity of coal and ashes from Figueira coal power plant in Brazil. J Radioanal Nucl Chem 2006;270(3):597–602. https://doi.org/10.1007/s10967-006-0467-0.
[92] Bem H, Wieczorkowski P, Budzanowski M. Evaluation of technologically enhanced natural radiation near the coal-fired power plants in the Lodz region of Poland. J Environ Radioact 2002;61(2):191–201.
[93] Charro E, Peña V. Environmental impact of natural radionuclides from a coal-fired power plant in Spain. Radiat Prot Dosimetry 2013;153(4):485–95. https://doi.org/10.1093/rpd/ncs126.
[94] Bureau of Indian Standard (BIS). Indian standards for industrial effluents. BIS: 2490-1974.
[95] Ward CR, French D, Jankowski J. Comparative evaluation of leachability test methods and element mobility for selected Australian fly ash samples. Cooperative Research Centre for Coal in Sustainable Development. Technical Note, 22; 2003.
[96] Jankowski J, Ward CR, French D. Preliminary assessment of trace element mobilisation from Australian fly ashes. Co-operative Research Centre for Coal in Sustainable Development. Research Report 2004;45:44.
[97] Dubikova M, Jankowski J, Ward CR, French D. Modelling mobility in water-flyash interactions. Co-operative Research Centre for Coal in Sustainable Development, Brisbane: Research Report, 61; 2006.
[98] Jones DR. The leaching of major and trace elements from coal ash. In Environmental aspects of trace elements in coal; Springer, Dordrecht, 1995:221-262.
[99] Kim AG, Kazonich G, Dahlberg M. Relative solubility of cations in class F fly ash. Environ Sci Technol 2003;37(19):4507–11.
[100] World Health Organization (WHO). Guideline for Drinking Water Quality, 4th ed. Geneva, Switzerland; 2011.
[101] Department of Environment (DoE). Industrial Effluents Quality Standard for Bangladesh, (Bangladesh Gazette Additional August, 28, 1997). The Environment Conservation Rules 1997. Government of the People's Republic of Bangladesh, Dhaka.
[102] Ramya SS, Deshmukh VU, Khandekar VJ, Padmakar C, SuriNaidu L, Mahore PK, et al. Assessment of impact of ash ponds on groundwater quality: A case study from Koradi in Central India. Environ Earth Sci 2013;69(7):2437–50.
[103] Rahman MM, Howladar MF, Hossain MA, Shahidul Huqe Muzemder ATM, Al Numanbakth MA. Impact assessment of anthropogenic activities on water environment of Tillai River and its surroundings, Barapukuria Thermal Power Plant, Dinajpur, Bangladesh. Groundw Sustain Dev 2020;10(November 2019). https://doi.org/10.1016/j.gsd.2019.100310.
[104] Howladar MF. An assessment of surface water chemistry with its possible sources of pollution around the Barapukuria Thermal Power Plant impacted area, Dinajpur, Bangladesh. Groundw Sustain Dev August 2015;2017(5):38–48. https://doi.org/10.1016/j.gsd.2017.03.004.
[105] Mandal A, Sengupta D. Radionuclide and trace element contamination around Kolaghat Thermal Power Station, West Bengal - Environmental implications. Curr Sci 2005;88(4):617–24.
[106] Spadoni M, Voltaggio M, Sacchi E, Sanam R, Pujari PR, Padmakar C, et al. Impact of the disposal and re-use of fly ash on water quality: The case of the Koradi and

Khaperkheda thermal power plants (Maharashtra, India). Sci Total Environ 2014; 479-480:159–70.
[107] Ruhl L, Vengosh A, Dwyer GS, Hsu-Kim H, Schwartz G, Romanski A, et al. The impact of coal combustion residue effluent on water resources: A North Carolina example. Environ Sci Technol 2012;46(21):12226–33.
[108] Harkness JS, Sulkin B, Vengosh A. Evidence for coal ash ponds leaking in the southeastern United States. Environ Sci Technol 2016;50(12):6583–92.
[109] Goodarzi F. Assessment of elemental content of milled coal, combustion residues, and stack emitted materials: Possible environmental effects for a Canadian pulverized coal-fired power plant. Int J Coal Geol 2006;65(1–2):17–25. https://doi.org/10.1016/j.coal.2005.04.006.
[110] Sajwan KS, Alva AK, Punshon T, Twardowska I (Eds.). Coal Combustion Byproducts and Environmental Issues; 2011. 242 p. New York, London, Springer.
[111] Amster E. Public health impact of coal-fired power plants: A critical systematic review of the epidemiological literature. Int J Environ Health Res 2021;31(5): 558–80. https://doi.org/10.1080/09603123.2019.1674256.
[112] Finkelman RB, Greb SF. Environmental and Health Impacts. Appl Coal Petrol. Published online 2008:263-287. doi:10.1016/B978-0-08-045051-3.00010-5.
[113] Finkelman RB, Orem WH, Plumlee GS, Selinus O. Applications of Geochemistry to Medical Geology. 2nd ed. Elsevier B.V.; 2018. doi:10.1016/B978-0-444-63763-5.00018-5.